Tectonophysics 610 (2014) 1–24

Contents lists available at ScienceDirect

Tectonophysics

journal homepage: www.elsevier.com/locate/tecto

Review Article

Invited review paper: Fault creep caused by subduction of rough seafloor relief

Kelin Wang [a,*], Susan L. Bilek [b]

[a] Pacific Geoscience Centre, Geological Survey of Canada, Natural Resources Canada, 9860 West Saanich Road, Sidney, British Columbia V8L 4B2, Canada
[b] Department of Earth and Environmental Science, New Mexico Institute of Mining and Technology, 801 Leroy Place, Socorro, NM 87801, USA

ARTICLE INFO

Article history:
Received 3 August 2013
Received in revised form 12 November 2013
Accepted 14 November 2013
Available online 27 November 2013

Keywords:
Megathrust earthquakes
Subducting topography
Fault creep
Fault zone structure
Fault slip behaviour

ABSTRACT

Among the wide range of thermal, petrologic, hydrological, and structural factors that potentially affect subduction earthquakes, the roughness of the subducting seafloor is among the most important. By reviewing seismic and geodetic studies of megathrust locking/creeping state, we find that creeping is the predominant mode of subduction in areas of extremely rugged subducting seafloor such as the Kyushu margin, Manila Trench, northern Hikurangi, and southeastern Costa Rica. In Java and Mariana, megathrust creeping state is not yet constrained by geodetic observations, but the very rugged subducting seafloor and lack of large earthquakes also suggest aseismic creep. Large topographic features on otherwise relatively smooth subducting seafloor such as the Nazca Ridge off Peru, the Investigator Fracture Zone off Sumatra, and the Joban seamount chain in southern Japan Trench also cause creep and often stop the propagation of large ruptures. Similar to all other known giant earthquakes, the Tohoku earthquake of March 2011 occurred in an area of relatively smooth subducting seafloor. The Tohoku event also offers an example of subducting seamounts stopping rupture propagation. Very rugged subducting seafloor not only retards the process of shear localization, but also gives rise to heterogeneous stresses. In this situation, the fault zone creeps because of distributed deformation of fractured rocks, and the creep may take place as transient events of various spatial and temporal scales accompanied with small and medium-size earthquakes. This process cannot be described as stable or unstable friction along a single contact surface. The association of large earthquakes with relatively smooth subducting seafloor and creep with very rugged subducting seafloor calls for further investigation. Seafloor near-trench geodetic monitoring, high-resolution imaging of subduction fault structure, studies of exhumed ancient subduction zones, and laboratory studies of low-temperature creep will greatly improve our understanding of the seismogenic and creep processes and their hazard implications.

Contents

* Corresponding author.

0040-1951/$ – see front matter.
http://dx.doi.org/10.1016/j.tecto.2013.11.024

1. Introduction

Understanding how the roughness of subducting seafloor affects subduction earthquakes is important for assessing seismic and tsunami hazards, but it is also a subject of debate. Interests in this subject have been renewed by the two most recent giant earthquakes ($M_w = 9$ or greater). The $M_w = 9.2$ Sumatra earthquake of 2004 put in doubt some of the widely held views about what controls the size of subduction earthquakes (Stein and Okal, 2007). It is thus relevant to ask whether the potential of any subduction zone to produce giant earthquakes is limited only by its length (McCaffrey, 2008). This translates to the question: Can some physical processes, particularly the subduction of topographical features, persistently limit earthquake size? After the $M_w = 9$ Tohoku earthquake of 2011, ideas were proposed to explain its long lapse time from its predecessor (~1100 years) and its large coseismic slip (~50 m or more) and tsunami. One idea is that a subducting seamount or some other geometrical anomaly strongly locked the megathrust for a long time and then produced unusually high coseismic stress drop (Duan, 2012; Kumagai et al., 2012; Zhao et al., 2011). This reopens an old question: Do subducting topographic anomalies generally cause strong locking and generate large earthquakes?

Global or regional syntheses generally argue for a negative correlation between very large earthquakes ($M_w > 8$) and subducting seafloor with large topographic reliefs (Kelleher and McCann, 1976; Kopp, 2013; Loveless et al., 2010; Morgan et al., 2008; Sparkes et al., 2010) or, equivalently, a positive correlation between large events and subducting seafloor smoothed by a large amount of sediments (Heuret et al., 2012; Ruff, 1989; Scholl et al., 2011). Case studies of individual earthquakes yield mixed results (Bilek, 2007). An $M_w = 7.8$ earthquake in 1994 in the Java subduction zone was thought to be caused by a subducting seamount (Abercrombie et al., 2001), but recent seismic imaging found no evidence for a subducting seamount in the rupture area (Shulgin et al., 2011). A seismically imaged subducting seamount at the Nankai subduction zone is reported to be a slip barrier that caused the rupture in an $M_w \approx 8.2$ earthquake in 1946 to halt before propagating farther along strike to generate a large tsunami (Cummins et al., 2002; Kodaira et al., 2000). A fracture zone in the subducting plate is reported to have stalled the rupture of the 2001 $M_w = 8.4$ earthquake off Peru then allowed it to continue its propagation along strike (Robinson et al., 2006). A subducting aseismic ridge caused a slip minimum in the 2007 $M_w = 8.1$ Solomon earthquake but allowed large slip to both sides (Chen et al., 2009; Furlong et al., 2009). In general, subduction earthquakes that are thought to be linked to subducting seamounts tend to be relatively small in size (Bilek et al., 2003) and/or feature rather complex rupture processes (Das and Watts, 2009) that often imply the involvement of multiple faults in different orientations (Wang and Bilek, 2011).

Discussions on this subject are normally focused on how geometrical irregularities influence coseismic rupture, commonly in terms of seismic "asperities" or "barriers." The location of the geometrical feature relative to the rupture is usually poorly defined. The conjugate question of how these irregularities influence interseismic locking has been addressed only on a few occasions. Mochizuki et al. (2008) studied earthquake activity over an 80-yr period around a well imaged subducting seamount near the southern end of Japan Trench and concluded that the seamount had been creeping aseismically while causing earthquakes in its neighbourhood, including a repeating sequence of M ~ 7 events slightly farther landward. Singh et al. (2011) described seismic imaging of a seamount to 30–40 km depths in a seismically quiet area of the Sumatra subduction zone and proposed that the seamount is subducting seismically. Wang and Bilek (2011) reasoned that subducting seamounts create favourable structural and stress environments for aseismic creep and small earthquakes.

This review article attempts to summarise the state of knowledge of this subject, addressing both observational and theoretical aspects. We do not attempt to cover the much broader subject of what controls subduction earthquake processes. Even for a very smooth fault, the slip and seismogenic behaviour must be influenced by a range of geological and geophysical factors such as the type of fault wall rocks, the amount and type of subducted sediments, temperature and pressure-controlled rheology, and fluid pressure in the fault zone. But here we focus only on the effects of geometrical irregularities of the fault zone due to uneven subducting seafloor. We describe seafloor of large topographic relief as being rugged or rough, different from the scale invariant roughness described by fractals (Turcotte, 1992). The issue of scale invariance will be discussed in Section 3.1.

The article is structured as follows. Section 2 is focused on modern observations. We review observations from subduction zones with extremely rugged subducting seafloor. Where available, we pay special attention to geodetic observations made over the past two decades that constrain the locking or creeping state of the plate interface. A mostly creeping fault segment is unlikely to be a primary candidate for the location of a future great earthquake. We will show that, where large topographic reliefs are subducted, geodetic observations consistently suggest interface creep, usually accompanied with numerous small and some medium size ($M < 7.5$) earthquakes. Section 3 is focused on physical concepts. We provide a critique of various models seen in the literature pertaining to how subducting geometrical irregularities stop or facilitate large earthquakes, with references to relevant studies in continental settings. At the end of Section 3, we explore the geology and mechanics of fault zone creep caused by geometrical irregularities with reference to fault zone structures of exhumed ancient subduction zones. Before summarising our conclusions, we discuss in Section 4 the role of subducting seamounts in the Tohoku earthquake.

2. Fault behaviour observed at subduction zones of very rugged incoming seafloor

If subducting seamounts or similar geometrical irregularities generally cause large earthquakes, they should cause locking of the subduction fault most of the time. Conversely, if they act as rupture barriers in large earthquakes, they must creep during the time between large earthquakes to balance the slip budget of the subduction fault. Here we review geodetic and earthquake studies from a number of

subduction zones featuring very rugged incoming seafloor. We summarise the geodetic results in terms of a "creeping ratio" κ, the rate of geodetically determined fault creep as a fraction of the long-term speed of plate subduction. The results suggest that creeping, instead of locking, is a common state of the fault at these subduction zones or segments.

We have selected subduction zones (or segments) that are extreme, end-member examples of rugged subducting seafloor (Fig. 1). In these places, no statistical measures (Mareschal, 1989; Morgan et al., 2008) are needed to verify the presence of large topographic reliefs on the incoming seafloor, and we infer that the subducted portion of the seafloor is similarly rugged. In some limited survey areas, geophysical imaging of subducted topographic features is available. Because the creeping ratio characterises average slip behaviour of a large portion of the plate interface, the results are not sensitive to the exact location of individual geometrical features. This is different from attempting to correlate one individual feature to one specific earthquake. Because of the theme of this review, we do not discuss the slip behaviour of subduction faults with smooth incoming seafloor. It is already well established that subduction of relatively smooth seafloor in some cases produces very large earthquakes but in other cases, such as the Shumagin segment of the Alaska subduction zone (Fournier and Freymueller, 2007), exhibits creep.

When the state of fault creep is inferred from Global Positioning System (GPS) observations, several issues should be kept in mind. (1) Except for two sites off Peru (Gagnon et al., 2005), all the GPS sites in studies reviewed here are located on land and have limited or no near-trench resolution. Therefore, the creeping/locking state of the near-trench part of the plate interface is poorly known or unknown at present. (2) The inference of fault locking/creep in these studies is based on an elastic dislocation model. The neglect of viscoelastic mantle behaviour is a source of uncertainties, but the problem is serious only if fault locking is predominant (Wang et al., 2012). (3) If a small patch of the fault is locked, the creep of its neighbouring fault area tends to slow down or stop. Because of this "stress shadowing" effect (Hetland and Simons, 2010), geodetically determined fault creep (or locking) should not be directly translated to frictional properties of the fault. (4) Inversion of geodetic data tends to yield sub-convergence creep, often called "partial coupling", that is, the fault is seen to be creeping at a rate lower than the rate of plate subduction ($\kappa < 1$). The mechanism responsible for this mode of fault motion, if true, is poorly understood and will be further discussed in Section 3.4.4. In some cases, it may simply be an average effect of mixed locked and creeping patches. Regardless of the mechanism, the creeping ratio is a useful indicator for whether the fault exhibits significant creep. (5) The history of using GPS to observe subduction faults is only about two decades long. It is reasonable to assume that the geodetically observed creeping, if it is not earthquake afterslip or slow slip events, is representative of a long-term behaviour, but the assumption cannot be observationally verified at present or in the immediate future.

Earthquake data are based on global catalogues to ensure a reliable comparison for all subduction zones. Because we are interested in earthquakes that occur on the megathrust, we select earthquake hypocenters from the Global Centroid Moment Tensor (GCMT, www.globalcmt.org) catalogue that have focal mechanisms with high (>45°) plunge values of the T axis and depths less than 100 km. Most, although not all, of the earthquakes that are not on the subduction megathrust are thus excluded from this selection. The GCMT catalogue is time-limited, containing events as early as 1976 through July 2013 as of this writing, but it provides a globally consistent catalogue of thrust events with moment magnitude (M_w) values that provide the best estimates of earthquake size. Hypocenters are centroid hypocenters, giving the location of the centroid, or centre, of moment release. We also examine the U.S. Geological Survey earthquake catalogue (www.earthquake.usgs.gov/regional/neic) that contains historical events to the early 1900s based on data from the National Oceanic and Atmospheric Administration (NOAA), especially at the largest magnitudes, but without consistently available focal mechanism information. Large events from this USGS catalogue are noted but weighted less in the regional discussions because of the uncertainty in their location.

2.1. Kyushu

The Kyushu margin (Fig. 2) is the westernmost segment of the Nankai subduction zone, southwest Japan. Here the Philippine Sea (PS) plate

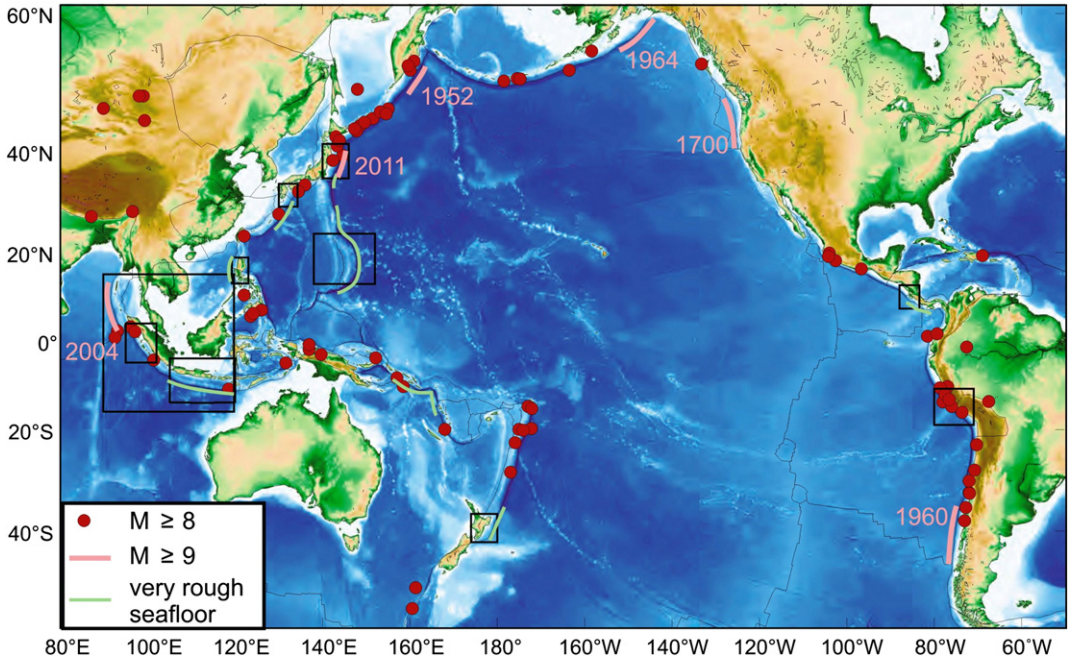

Fig. 1. World map showing general lack of correlation between rugged subducting seafloor and great megathrust earthquakes and showing locations of map areas of Fig. 2 through 10 and 14. Rupture extents of giant ($M_w \geq 9$) events are indicated with pink lines. Epicentre locations of other great ($M_w \geq 8$) events are from the USGS/NOAA catalogue for the time period of 1903–2012.

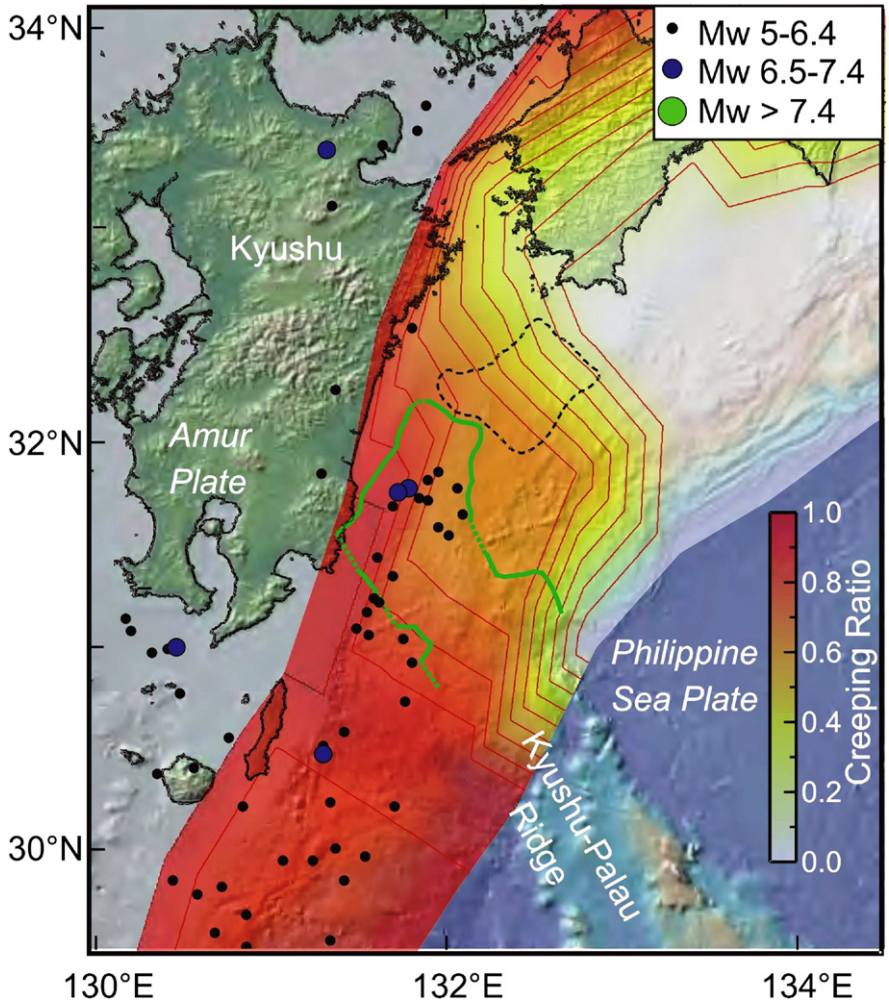

Fig. 2. Creeping state and seismicity of the Kyushu segment of the Nankai subduction zone, southwest Japan. Megathrust creeping ratio (contoured at 0.1 internal) is from the model of Wallace et al. (2009a); the seaward boundary of the model area approximately follows the trench. Green line is the outline of the subducted portion of the Kyushu–Palau ridge defined by Yamamoto et al. (2013). Black dashed line outlines the rupture area of the 1968 Hyuga-nada earthquake (Yagi et al., 1998), the largest megathrust event recorded in this area (Japan Meteorological Agency magnitude 7.5).

subducts beneath the Amur plate (also referred to as a breaking-away block of the Eurasia plate) at a rate of about 58 mm/yr in a nearly margin-normal direction (DeMets et al., 2010). South of Kyushu is the Ryukyu subduction zone, and the upper plate transitions into the Yangtze plate (or block). Back-arc rifting takes place in the Okinawa Trough, causing the Ryukyu Arc to move as an independent microplate (e.g., Bird, 2003). The Okinawa Trough rifting continues northward into Kyushu, roughly coinciding with the landward extension of the Kyushu–Palau ridge shown in Fig. 2, and GPS suggests that the forearc in Kyushu is undergoing active internal deformation (Nishimura and Hashimoto, 2006; Wallace et al., 2009a). Wallace et al. (2009a) suggest that the collision of the Kyushu–Palau ridge with the subduction margin leads to shear and fragmentation of the Kyushu forearc.

The Kyushu–Palau ridge is a pronounced bathymetric feature on the incoming seafloor. It is the remnant arc of the spreading centre of Shikoku basin active during ~30–15 Ma (Okino et al., 1999). Based on seismic imaging, the leading edge of the subducted portion of the Kyushu–Palau ridge has reached about 30 km depth beneath the continental shelf very near the coast (Yamamoto et al., 2013) (Fig. 2). Its subduction has caused strong structural disruption to the frontal forearc and produced many small and a few medium-size earthquakes (Park et al., 2009). Because of its oblique orientation, its point of entry into the subduction zone is not fixed but has swept through a significant part of the margin (Mahoney et al., 2011).

Seismicity within the Kyushu megathrust region is limited to events up to $M_w = 6.7$ based on the GCMT catalogue, $M_w = 6.9$ in the USGS catalogue, but up to $M_w = 7.5$ based on studies using the local seismic network (Shiono et al., 1980). The majority of events most clearly linked with the subduction megathrust occur in the central and southern segments of the margin, from the intersection of the Kyushu–Palau ridge and southward. Large thrust events ($M_w = 6–7.5$) occurred either to the side of the subducted Kyushu–Palau ridge or ahead of its leading edge (Yamamoto et al., 2013). Within the historical USGS/NOAA catalogue that dates back to the early 1900s, there are 3 events with larger magnitude that may have occurred on the megathrust based on catalogue hypocenter. These events (1931 M 7.5, 1941 M 7.9, and 1968 M 7.8) have catalogue locations that overlap with the central region of moderate magnitude events in the GCMT catalogue, but there are large uncertainties in their locations, focal mechanisms, and magnitudes.

The Japanese islands are covered by the continuously monitoring GPS network GEONET with site spacing of 20–50 km. Wallace et al. (2009a) inverted GPS velocities from 265 of these sites based on data from 1996 to 2004 to obtain the creeping ratio distribution shown in Fig. 2. To account for permanent intraplate deformation, Wallace et al. (2009a) divided the upper plate into a few blocks and estimated the block motion parameters simultaneously with the locking state of the subduction fault. The results show the Kyushu segment to be creeping

at 60% to 100% of the subduction rate, in contrast with the segment to the northeast at the Nankai Trough.

Because of the large distance of the GPS sites from the trench, neither the narrow near-trench strip of full locking between latitudes 31° and 32° nor the near-trench full creep farther south can be resolved. However, the dramatic along-strike variations in the overall creeping state is a robust result, since there is no systematic change in GPS site density and trench-coast distance. This variation is consistent with the long-standing notion based on written history of the past thirteen centuries that subduction at the Kyushu segment is largely aseismic with only small and medium size earthquakes, but the rest of the Nankai margin repeatedly produces great earthquakes (Ando, 1975). The very high degree of locking along the rest of the Nankai margin has been confirmed time and again by analyses of geodetic observations (e.g., Yoshioka and Matsuoka, 2013). The lack of significant locking at Kyushu has also been recognised in other geodetic studies. Inversion of GPS velocities by Nishimura and Hashimoto (2006) and Hashimoto et al. (2009a) indicates a mostly creeping fault at Kyushu. Nishimura and Hashimoto (2006) derived strain rates from GEONET GPS data and found no evidence for active margin-normal shortening which would be expected if the subduction fault were significantly locked. Yamamoto et al. (2013) propose that the creeping is related to the subduction of the Kyushu–Palau ridge and the extensive structural damage it causes.

2.2. Manila Trench

At the Manila Trench, the seafloor of South China Sea is subducting beneath the Luzon archipelago in an easterly direction (Fig. 3). South China Sea is part of the Sunda block (also referred to as the Sundaland plate), a large portion of the Eurasia (EA) plate that moves somewhat independently. Luzon belongs to the Philippine Sea (PS) plate but is part of a broad deformation zone that accommodates some of the Sunda-PS convergence. There is difficulty in constraining subduction rate at the Manila Trench because of the long-term upper plate deformation, but recent GPS measurements (Galgana et al., 2007; Yu et al., 2013) generally support the tectonic model of Rangin et al. (1999). According to the estimates of Hsu et al. (2012), the subduction rate is about 80–100 mm/yr around latitude 20° and decreases southward to 50–60 mm/yr around 14°, but the rate in the south is much lower according to the estimates of Galgana et al. (2007).

The most pronounced bathymetric feature of the incoming plate is the Scarborough seamount chain (Fig. 3), the remnant of an E–W trending spreading centre that stopped spreading some 17 Ma ago (Taylor and Hayes, 1983). The subduction of many seamounts causes large variations in the geological structure of the frontal forearc over short distances (Hayes and Lewis, 1984). To the north, the incoming seafloor is seemingly smooth. However, seismic surveys conducted just north of the map area of Fig. 3 reveal very rugged volcanic basement beneath a sediment cover of 1–2 km (Ku and Hsu, 2008; Li et al., 2013). Some of the seamount-like features still stand above the seafloor by a few hundred metres despite the thick sediment layer, suggesting a total height of at least 2 km. Extensive faulting of the frontal forearc is probably related to the subduction of these features (Ku and Hsu, 2008; Li et al., 2013).

The Manila Trench subduction zone produces numerous small earthquakes. Based on data within the GCMT catalogue, the largest thrust mechanism earthquake within the area of Fig. 3 is the 1977 March 18 $M_w = 7.2$ Luzon event, but it cannot be a megathrust event because it is located too far east. Within the potential seismogenic zone, the largest event is less than $M_w = 6.5$. Historical and geological

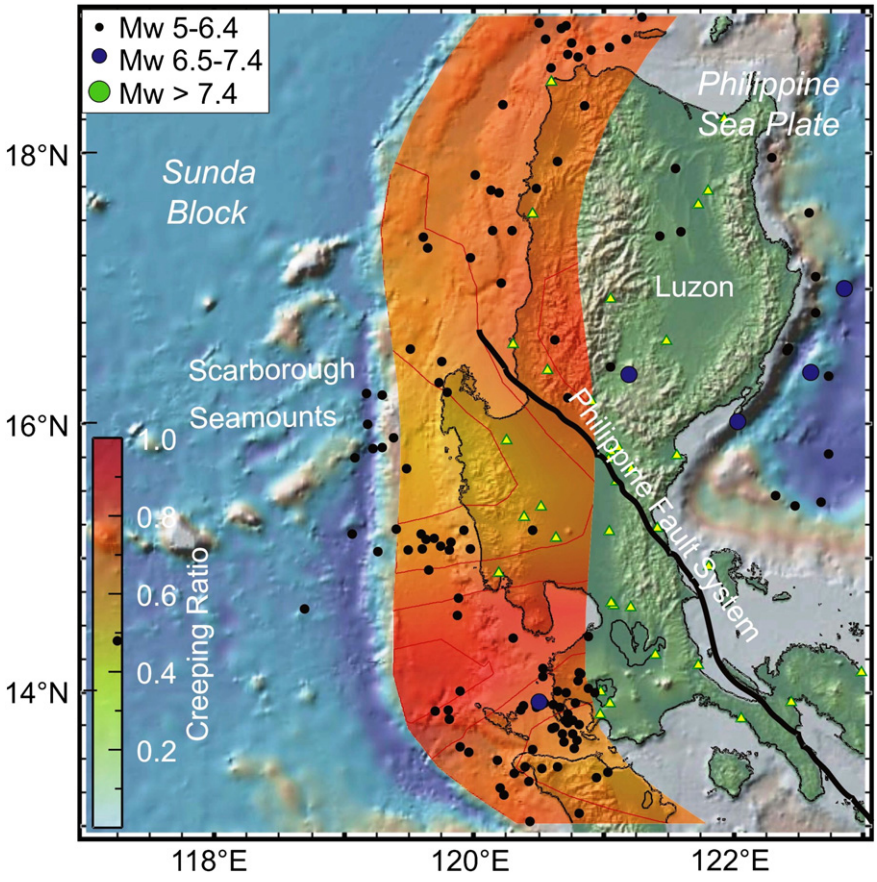

Fig. 3. Creeping state and seismicity of the Manila Trench. Megathrust creeping ratio was determined by Hsu et al. (2012) by inverting GPS data from shown sites (triangles); Galgana et al. (2007) reported almost 100% creeping based on similar data.

evidence for past great subduction earthquakes and tsunamis in this region is scarce and controversial (A. Switzer, personal communication, 2013). A better understanding of the likelihood of a great earthquake of M_w ~ 9 along the Manila Trench is important however, because large tsunami waves can inundate the coastal areas of Luzon, Taiwan, and Chinese mainland (Megawati et al., 2009; Wu and Huang, 2009).

The creeping/locking state of the shallow, potentially seismogenic part of the subduction fault has been inferred from land-based GPS measurements. The creeping ratio shown in Fig. 3 was obtained by Hsu et al. (2012) by inverting GPS velocities at sites shown also in Fig. 3 (triangles). In this model, the creeping ratio in the area of seamount subduction is about 60%. Galgana et al. (2007) also estimated the creeping ratio of the Manila Trench from GPS measurements, as part of a large regional study. They obtained an average value of 99% ± 2% which means creeping at full rate (not shown in Fig. 3).

The difference between these two estimates is not due to use of different data. The GPS velocities inverted by Hsu et al. (2012) were determined by Yu et al. (2013) using measurements spanning the period 1996–2008. Galgana et al. (2007) included earlier measurements (up to 2002) from most of the same sites but also data from some additional sites. The GPS velocity fields obtained by the two groups are very similar, although those by Yu et al. (2013) may have smaller uncertainties because of the longer observation period. The difference in the creeping ratios must be due to the different approaches used to deal with long-term upper plate deformation. Galgana et al. (2007) divided the upper plate into six blocks and determined the slip rates of all the block boundaries and the subduction fault simultaneously. Hsu et al. (2012) assumed a single elastic upper plate but, before inversion, corrected GPS velocities for the motion of one of the major crustal faults, the Philippine fault that approximately divides the Luzon Island into two halves (Fig. 3). Hsu et al.'s (2012) model systematically overestimates the magnitude of GPS velocities relative to the Sunda block for sites away from the west coast (see Fig. 3b of Hsu et al. (2012)), reflecting an overestimate of the rate of margin-normal shortening. This combined with an overestimate of the subduction rate could lead to an overestimate of the slip deficit rate of the megathrust, that is, an underestimate of the creeping ratio. The creeping ratio shown in Fig. 3 therefore represents a lower bound.

The sparse distribution of GPS sites and their large distance from the trench preclude resolving greater details. However, if there were significant locking of the plate interface over a downdip width of 50–100 km, the sites about 100 km from the trench would have detected it. In both studies, the reliability of the creeping ratio deteriorates towards the north because of the decreasing number of GPS sites. The creeping state of the shallowest near-trench part of the fault is unconstrained.

2.3. Northern Hikurangi

The Hikurangi margin (Fig. 4) is the southernmost segment of the ~3000 km long Tonga–Kermadec–Hikurangi subduction zone system, where the Pacific (PA) plate subducts beneath the Australia (AU) plate in a westerly direction. Active rifting occurs in the Kermadec back arc. Crustal extension continues into the North Island of New Zealand in the form of intra-arc rifting but diminishes southward, such that the Hikurangi forearc rotates clockwise with respect to stable AU. As a result of the forearc rotation and shear, the relative motion between PA and Hikurangi forearc is margin-normal with rates decreasing from about 60 mm/yr off the northeastern tip of the North Island to less than 20 mm/yr off the southern tip (Wallace et al., 2004). To the south, the

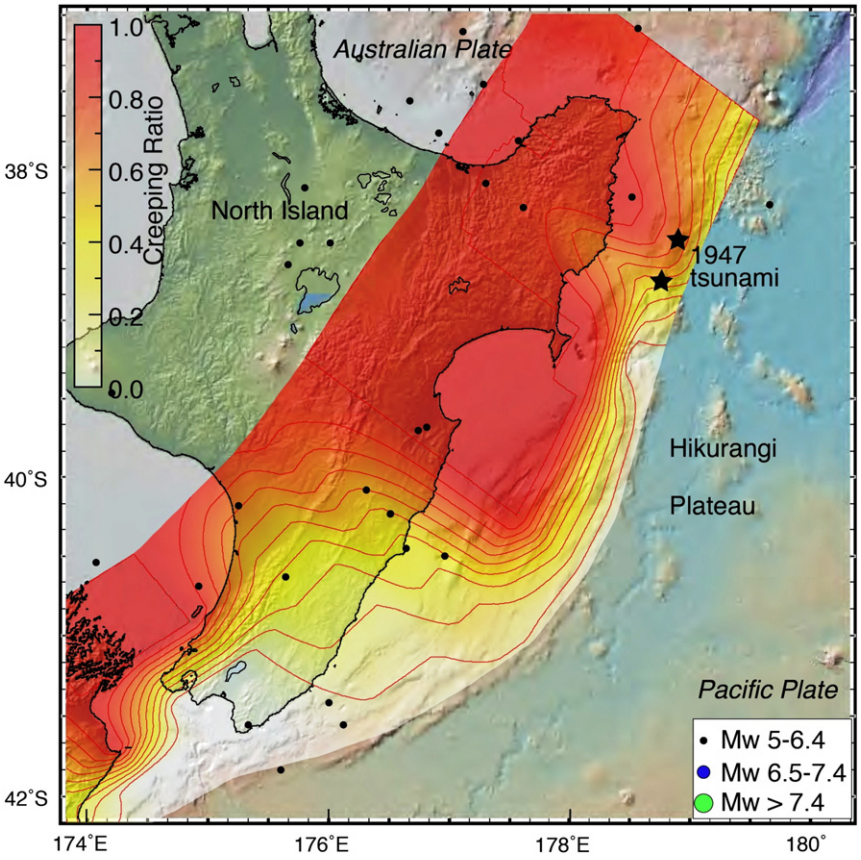

Fig. 4. Creeping state and seismicity of the Hikurangi subduction zone. Megathrust creeping ratio is from Wallace et al. (2004, 2009b), based on average GPS velocities over many years. The creep in northern Hikurangi actually takes place as discrete slow slip events (Wallace and Beavan, 2010). Approximate locations of two 1947 events, interpreted by some to be tsunami earthquakes, are from Doser and Webb (2003).

Chatham Rise on the Pacific plate collides into the South Island, and subduction transitions to collision.

The subducting seafloor is that of the Hikurangi plateau, featuring a very rugged surface (Fig. 4). The sediment thickness on the incoming seafloor is less than 1 km off northern Hikurangi but increases to 3–5 km to the south. The thick sediment pile at southern Hikurangi makes the megathrust in that area much smoother. At northern Hikurangi, a number of subducting seamounts have been seismically imaged (Barker et al., 2009; Bell et al., 2010). They are seen to cause large perturbations to the overriding plate, giving rise to a complex internal structure of the subduction fault.

Knowledge of past subduction earthquakes at the Hikurangi margin is fairly limited due to the short historical record (~150 years) in New Zealand. The maximum magnitude for an event in the GCMT catalogue is $M_w = 6.4$. The best documented megathrust event of significant size is the Mw = 5.6 Gisborne earthquake of 1966 (Webb and Anderson, 1998). Two events in 1947 in the historical USGS/NOAA catalogue have magnitude estimates of 6.9–7.1 and were located near the trench (Fig. 4). These two events have been classified by some as tsunami earthquakes, producing larger tsunami than expected and having source properties classified as slow, such as long duration and dominantly low frequency seismic radiation (e.g. Doser and Webb, 2003).

Wallace et al. (2004) inverted GPS velocities at about ~350 sites to determine the secular motion of a number of upper plate blocks and interseismic locking of the Hikurangi subduction fault. The GPS data were obtained from 24 regional campaign surveys in different time windows between 1991 and 2003. Site distribution in the eastern half of North Island was rather dense and even (not shown in Fig. 4). Later measurements, mostly using continuous GPS monitoring, verified earlier campaign measurements (Wallace and Beavan, 2010). The creeping ratio distribution in Fig. 4 is an updated version of the model of Wallace et al. (2004) as presented by Wallace et al. (2009b). It shows that off northern Hikurangi where a very rugged seafloor is subducting, the subduction fault is mostly creeping, in contrast to the locked segment further south. Again, because of the large distance from the GPS network to the trench, the creeping state of the shallowest, near-trench part of the subduction fault is largely unconstrained. However, similar to Nankai (Fig. 2), the large along-strike variation in the creeping ratio is a robust result. This variation, together with the interface creep of northern Hikurangi, has been verified by Lamb and Smith (2013) who inverted GPS velocities from continuously monitoring sites only but using a simpler model that did not involve several crustal blocks.

Continuous GPS monitoring at the northern Hikurangi margin has detected a number of shallow slow slip events (SSE) offshore of the east coast (Wallace and Beavan, 2010). For a given location, these events occur about every two years, each lasting several days to weeks and with a few to over 15 cm of slip. The creeping ratio shown in Fig. 4 is an average of several years or longer. The detection of many SSE events demonstrates that this "long-term" creep is accomplished mostly by episodic aseismic slip pulses. By inverting GPS velocities between SSEs, Wallace and Beavan (2010) show that the degree of locking of the plate interface would be much higher (nearly fully locked) had there not been these SSEs. With land-based geodetic measurements, the SSEs are seen to occur offshore, but it is not known at present whether they extend all the way to the trench. To estimate the potential of very shallow tsunami events, it is important to conduct near-field seafloor geodetic measurements to test the near-trench-locking hypothesis portrayed in Fig. 4.

2.4. Costa Rica

At the Costa Rica margin (Fig. 5), the Cocos plate subducts beneath the Caribbean plate at a rate of about 85 mm/yr (DeMets et al., 2010). Convergence at the Nicoya Peninsula and further northwest is slightly oblique, with the right-lateral component partially accommodated by a margin-parallel translation of a forearc sliver, although the landward boundary of the sliver is not geologically defined (Feng et al., 2012;

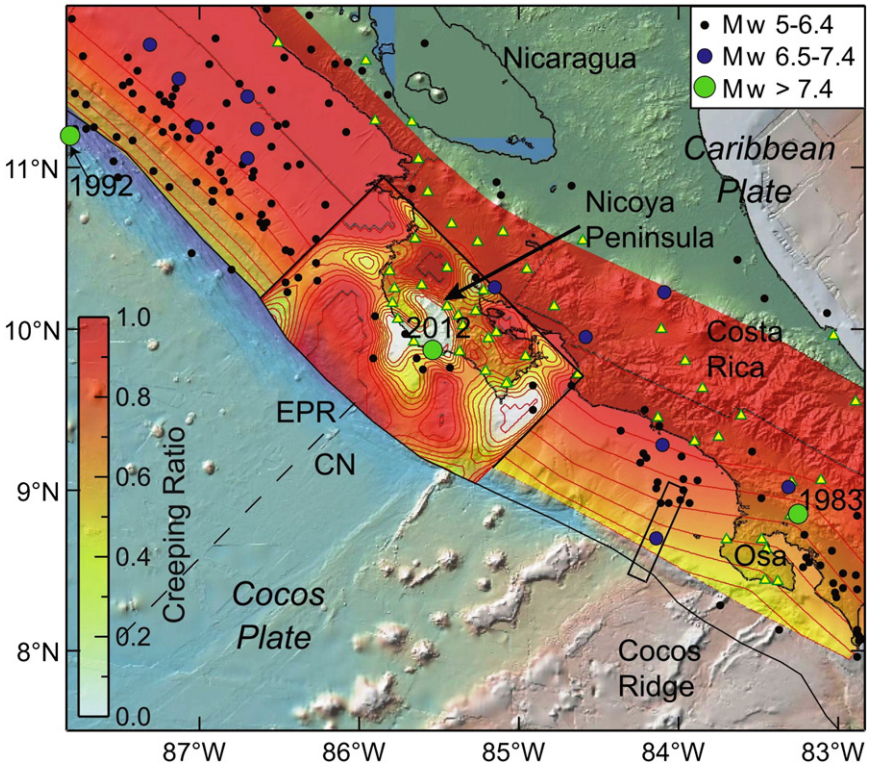

Fig. 5. Creeping state and seismicity of the Costa Rica margin. The smooth regional megathrust creeping ratio distribution was determined by LaFemina et al. (2009) using data from most of the shown GPS sites (triangles). The more detailed distribution for the Nicoya Peninsula area including the location of the 2012 earthquake was determined by Feng et al. (2012) using GPS data from that area. Box northwest of Osa Peninsula is the location of 3D seismic survey that shows numerous fractures due to seamount subduction (Kluesner et al., 2013). Dashed line off Nicoya is the "rough-smooth" boundary that divides rougher and smoother seafloors created at the Cocos–Nazca (CN) and East Pacific Rise (EPR) spreading centres, respectively.

Norabuena et al., 2004). The resultant Cocos — forearc convergence is less oblique. Southeast of the Nicoya Peninsula, the upper plate experiences large internal deformation and transitions to the Panama block of the Caribbean plate.

The northwest and southeast parts of the subducting plate were created at the East Pacific Rise (EPR) and Cocos–Nazca (CN) spreading centres, respectively. The boundary in between is referred to as the rough–smooth boundary (Fig. 5), but extreme bathymetric roughness of the CN-generated seafloor occurs ~60–70 km farther southeast. The Cocos ridge, formed as a result of the interaction of the Galapagos hot spot with the Galapagos spreading centre some 12.5–14.5 Ma ago (Harpp et al., 2005), and the many seamounts on both sides make the subducting seafloor one of the most rugged. Subduction of the extremely rugged seafloor has caused pervasive long-term deformation of the upper plate including regional uplift and extensive fracturing and faulting (Sak et al., 2009; Vannucchi et al., 2006; Zhu et al., 2009). Seamount subduction causes numerous fractures in the frontal forearc as identified in a recent three-dimensional (3D) seismic survey (Fig. 5) (Kluesner et al., 2013). Many re-entrants on the lower continental slope marked by recently subducted seamounts are clearly visible even at the relatively low resolution of Fig. 5. Better bathymetric images of the re-entrants can be found in, for example, Ranero and von Huene (2000) and Ranero et al. (2008).

The seismicity along the Costa Rica and Nicaragua regions is dominated by small to moderate magnitude events that are well distributed along the margin. There have been three large megathrust events in the GCMT catalogue, the 1992 $M_w = 7.6$ Nicaragua tsunami earthquake in the near-trench region off the coast of Nicaragua, the 2012 $M_w = 7.6$ Nicoya Costa Rica earthquake, and the 1983 $M_w = 7.4$ Osa event opposite the subducting Cocos Ridge. Rupture complexity, as described for the slip distributions for the 1992 and 1983 events, was linked to the nature of the subducting Cocos plate in the respective areas, and subducting seamounts might have been responsible for some of these and other smaller events (Bilek et al., 2003; Wang and Bilek, 2011).

In anticipation for an M ~ 7.8 megathrust earthquake beneath the Nicoya Peninsula, a very dense GPS network including continuous and campaign stations was developed since 1996, but there are fewer sites elsewhere (Fig. 5). Using data collected during 1996–2010 from 49 sites of the dense Nicoya network, Feng et al. (2012) determined a detailed megathrust creeping ratio distribution for that area (Fig. 5). The results indicate a mostly creeping megathrust with small patches of full locking. The anticipated earthquake eventually occurred in September 2012, with a slightly lower magnitude but a rupture zone roughly coinciding with the fully locked zone (zero creeping ratio) of Feng et al. (2012) beneath the Nicoya Peninsula (Protti et al., 2013). Using data collected during 1993–2005 from the regional network including many of the Nicoya sites, LaFemina et al. (2009) determined a much smoothed version of the creeping ratio distribution (Fig. 5). The creeping ratio is shown to be about 40%–80% across the shallow seismogenic part of the fault. If dense, near-field measurements were uniformly available, this smooth "partial locking" could turn out to be a low-resolution version of interspersed patches of locking and creep similar to what is shown by Feng et al. (2012) for Nicoya.

The Nicoya and Osa peninsulas are unusual in that the trench-coast distance is very small so that much of the megathrust seismogenic zone is directly beneath the land-based GPS network. The overall creeping behaviour estimated for these areas is most reliable. LaFemina et al. (2009) infer somewhat slower creep at Osa (Fig. 5) because the GPS data indicate slightly faster forearc shortening in the margin-normal direction. However, as explained by Gardner et al. (2013), the shortening here is primarily permanent upper-plate deformation associated with seamount subduction, not elastic strain accumulation due to interseismic locking. The creeping ratios are least reliable in the northwest part of Fig. 5 off Nicaragua where GPS sites are sparse and far from the trench. If the shown faster creep in that area of relatively smooth incoming seafloor is verified by future measurements, it will be another example to show that smooth faults can also creep (see discussions in Section 3.4.1). The important message of the Costa Rica observations is that the very rugged subducting seafloor here is not causing full locking.

2.5. Nazca Ridge off Peru

The earthquake history of the subduction boundary from northern Peru to southern Chile has been extensively studied (see review by Bilek, 2010). Sparkes et al. (2010) compared the rupture zones of thirteen $M_w > 8$ interplate earthquakes along this margin since 1868 with the bathymetry of the incoming plate. They found a good correlation between the rupture limits of these events and bathymetric reliefs >1000 m. Loveless et al. (2010) studied seismological and geodetic observations of six $7 < M_w < 8.5$ interplate earthquakes that occurred during 1995–2007 and examined their correlation with a number of geological and geophysical factors. They concluded that the locations and rupture extents of these earthquakes cannot be controlled by a uniform mechanism, but they noticed a strong correlation between slip patterns and gravity gradients in the forearc and between rupture limits and large morphological features.

We focus on the slip behaviour of the interface in response to the largest bathymetric feature on the incoming seafloor, the Nazca Ridge off Peru (Fig. 6). Here the Nazca plate subducts beneath South America at a rate of about 62 mm/yr in a direction almost due east, at a large angle to the margin-normal direction. The Nazca Ridge is oriented at about 45° with the direction of plate convergence, such that its entry point into the subduction zone has swept hundreds of kilometres of the margin, strongly affecting upper plate tectonics (Clift et al., 2003; Espurt et al., 2007; Hampel, 2002). The surface of the Nazca Ridge is jagged, featuring many seamounts often penetrating the 300–400 m sediment cover (Hampel et al., 2004).

Seismicity along this portion of Peru is heterogeneous, with maximum magnitudes of up to $M_w = 8.4$. Two earthquakes (2007 $M_w = 8.0$ and 1996 $M_w = 7.7$) occurred adjacent to the Nazca Ridge without significant rupture through the ridge (e.g. Bilek, 2010; Swenson and Beck, 1999). One older event in 1942 ($M_w = 8.1$) also occurred on the flank of the Nazca Ridge, but its rupture area is more poorly known (Swenson and Beck, 1996). Other large events occurred to the south of the Nazca Ridge between 17.5–18°S (2001 $M_w = 8.4$ and 2001 $M_w = 7.6$). Sparkes et al. (2010) found the subducting Nazca Ridge to be most potent in stopping large ruptures.

Through analyses of interseismic GPS observations, Perfettini et al. (2010) and Chlieh et al. (2011) found the subducting Nazca Ridge to be creeping, despite stress shadowing from its neighbouring segments that exhibit significant locking. To determine the creeping ratio in Fig. 6, Chlieh et al. (2011) had 87 GPS sites for their vast study area including northern Chile. Compared with the four regions discussed in Sections 2.1 through 2.4, the site distribution is rather sparse, and there is little resolution for the downdip distribution of the creeping ratio. The two seafloor GPS measurements around latitude 12.2°S (Gagnon et al., 2005) (Fig. 6) suggest that the apparent near-trench fast creep for most of the study area may be an artefact resulting from lack of near-field observations. However, of first-order importance is the along-strike variation in the creeping ratio and its striking correlation with the subducting bathymetry. The coastal GPS sites right above the subducting Nazca Ridge are only about 100 km from the trench. If there were significant locking over a fault width of 50–100 km, these sites would readily detect it. The significant numbers of small to moderate magnitude events within the catalogue primarily occur within high creep areas.

2.6. The Investigator Fracture Zone off Sumatra

The Sumatra margin (Fig. 7) has hosted a number of great earthquakes. The history of megathrust earthquakes including those since

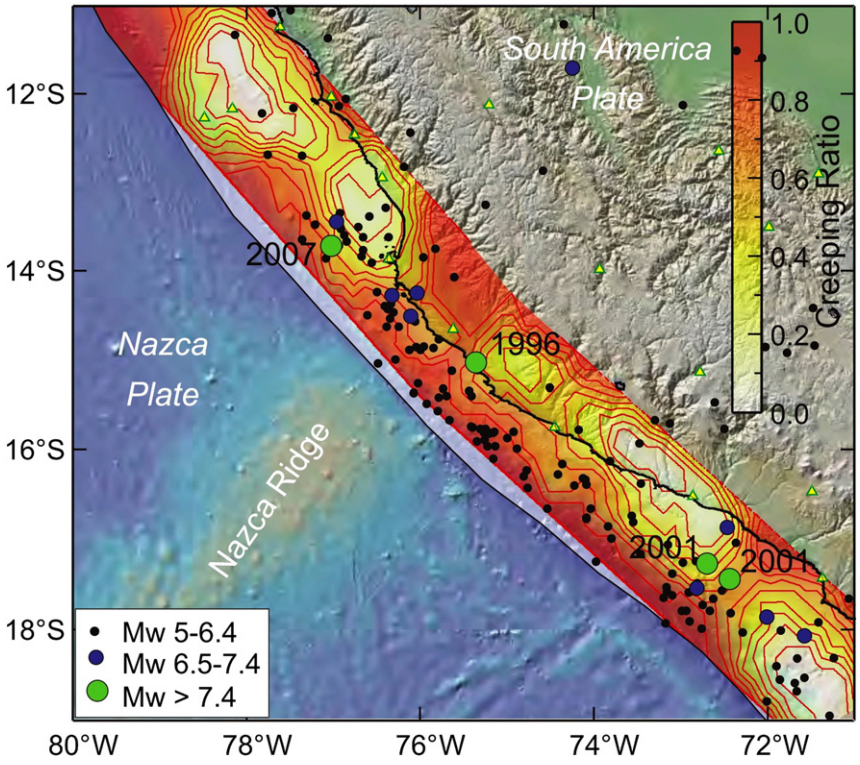

Fig. 6. Creeping state and seismicity related to the subduction of the Nazca Ridge at the Peru margin. The megathrust creeping ratio was determined by Chlieh et al. (2011) using GPS data from shown sites (triangles). Values northwest of 12°N should be ignored because of no GPS coverage.

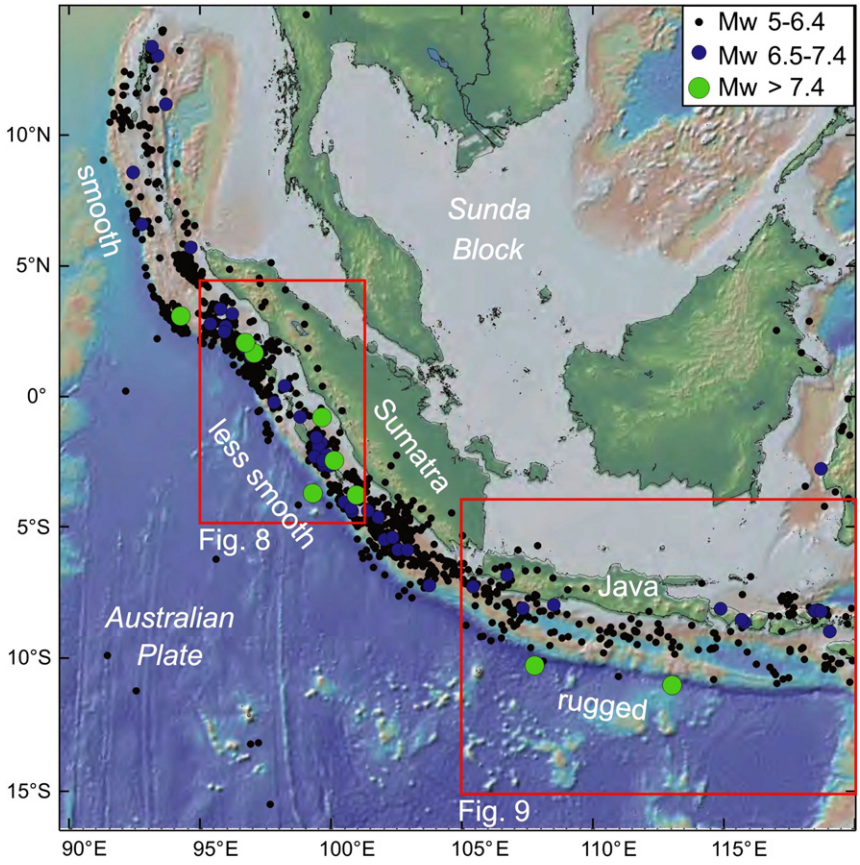

Fig. 7. The Sumatra–Java subduction zone showing along strike variations in seismicity and roughness of incoming seafloor. The northernmost segment with smooth subducting seafloor hosted the 2004 giant earthquake. The less smooth segment produced many large and great earthquakes. The rugged Java area has produced few large events. Red boxes indicate map areas of Figs. 8 and 9.

the devastating $M_w = 9.2$ event in 2004 has been summarised in a number of publications (e.g., Meltzner et al., 2012). There appear to be some persistent boundaries that tend to limit the along-strike length of megathrust earthquakes (Chlieh et al., 2008; Kopp, 2013; Meltzner et al., 2012). Similar to the Peru–Chile margin, the role of subducting bathymetric features in causing some of these boundaries is a subject of active research.

We focus on the megathrust slip behaviour in the area where the Investigator Fracture Zone (IFZ) is subducting (Fig. 8). Here the Australia plate converges with the Sunda block at about 60 mm/yr in a direction roughly 50° to strike. The right-lateral component is nearly fully accommodated by the strike-slip Sumatra fault that runs approximately along the volcanic arc, so that the AU subduction beneath the forearc is margin-normal. The IFZ is also referred to as the Investigator Ridge owing to its bathymetric expression. In high-resolution bathymetry (Kopp, 2013), the IFZ entering the Sumatra trench consists of four individual ridges of 5–40 km base width ranging 1.1–1.9 km in height above surrounding trench seafloor, topped with volcanic edifices (Fig. 8 inset).

The 2004 $M_w = 9.2$ event is the largest event in the historical catalogue for the Sumatra margin, with previous great events suggested based on various palaeoseismic data sets (e.g. Meltzner et al., 2012). Here we focus on earthquakes occurring in the region to the south of the 2004 rupture, primarily in the region of the IFZ. The largest thrust mechanism events along this portion of the margin occurred north of the IFZ (the 2005 $M_w = 8.6$ event) and south of the IFZ (the 2007 $M_w = 8.5$ event). There is significant small and moderate magnitude seismicity along much of the margin, however in the area of IFZ subduction, the seismicity diminishes.

Prior to the 2004 and 2005 great earthquakes, there had been over a decade of GPS measurements in Sumatra and its forearc islands (Bock et al., 2003). There had also been estimates of vertical crustal motion based on analysis of coral growth rings over half a century (Natawidjaja et al., 2004, 2007). Chlieh et al. (2008) inverted 33 GPS velocities derived from campaign data of 1991–2000 and 44 coral uplift/subsidence estimates to obtain the creeping ratio distribution shown in Fig. 8. Similar to other subduction zones, the creeping state for the near-trench area should be ignored, but the along-strike variations are robust results. The results show the area of IFZ subduction to be creeping at 60–100% of subduction rate, despite being partially in the stress shadow of large locked patches on both sides. The IFZ creep zone is approximately the southern rupture limit of the 2005 $M_w = 8.7$ Nias earthquake (Briggs et al., 2006) and northern limit of the 2010 $M_w = 7.8$ Mentawai tsunami earthquake (Hill et al., 2012) and perhaps of an $M_w \sim 8.4$ event in 1797 (Meltzner et al., 2012).

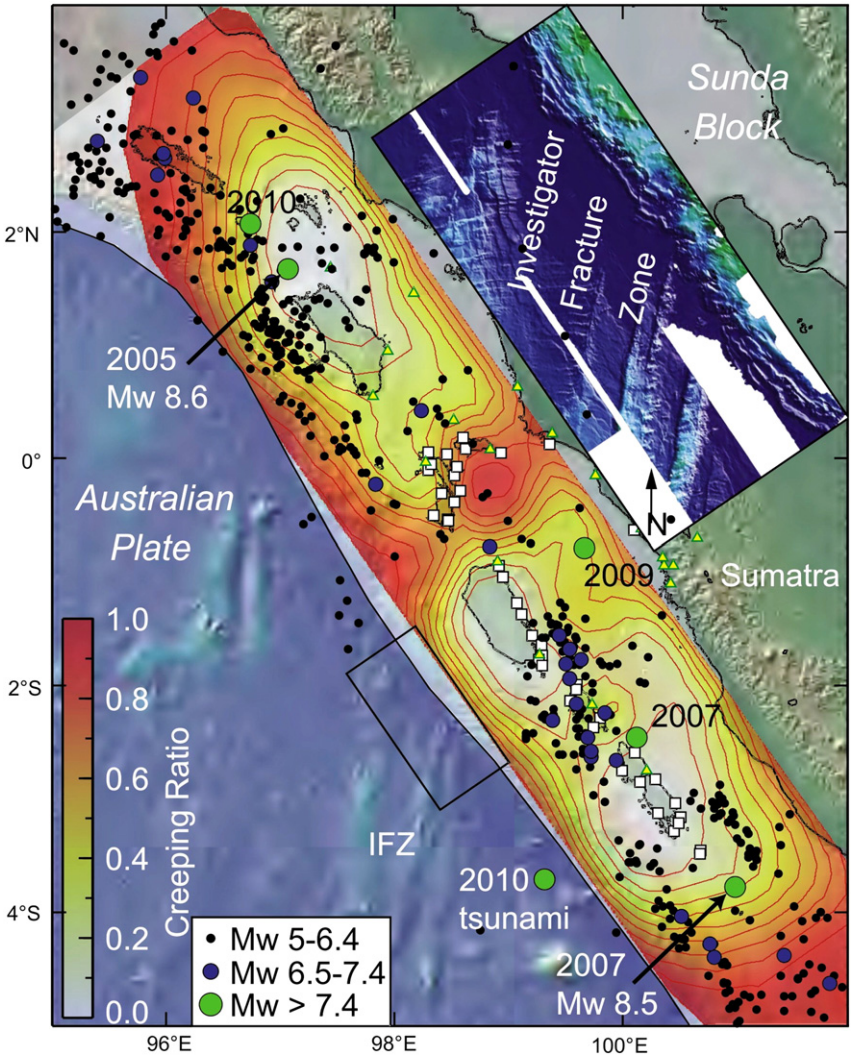

Fig. 8. Creeping state and seismicity related to the subduction of the Investigator Fracture Zone at the Sumatra margin. The megathrust creeping ratio distribution was determined by Chlieh et al. (2008) using GPS data (sites shown as triangles) and coastal coral growth data (sites shown as squares). Inset shows high-resolution bathymetry for the IFZ subduction area from Kopp (2013) for the rectangular area indicated on the main map (about 1.5°S–3°S).

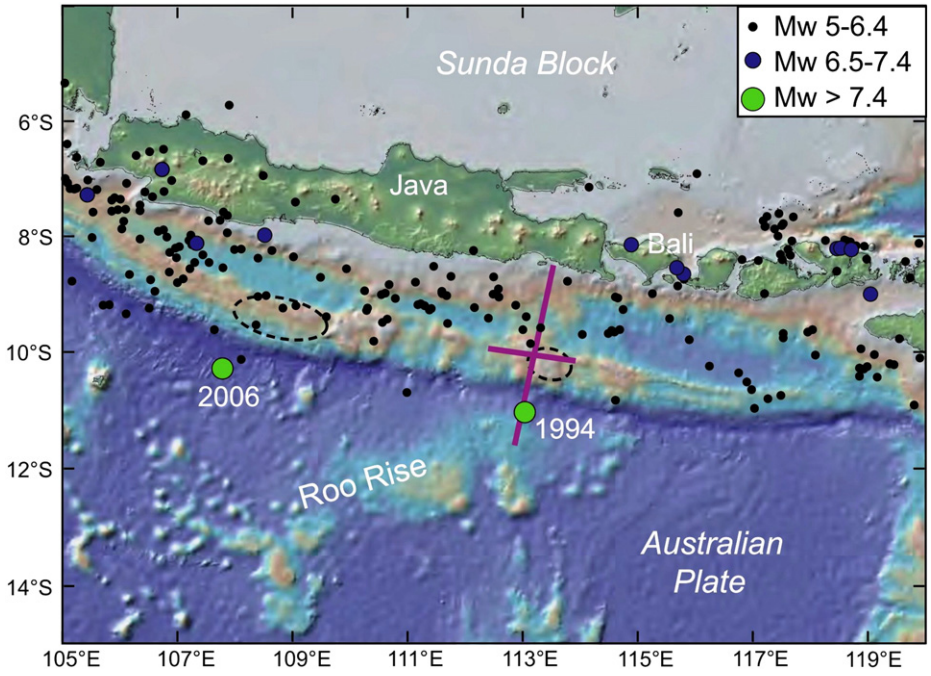

Fig. 9. Seismicity of the Java margin, traditionally considered to be a creeping subduction zone. The GCMT centroid locations of the tsunami earthquakes of 1994 and 2006 indicate the very shallow source of moment release, with their epicentres plotted seaward of the trench with higher errors. The more accurately determined rupture zones of these events are outlined using dashed lines north of the trench (Abercrombie et al., 2001; Bilek and Engdahl, 2007). Pink lines represent the two crossing seismic survey profiles that showed the absence of a subducting seamount in the 1994 rupture area (Shulgin et al., 2011).

2.7. Java

At the Java subduction zone (Fig. 9), the Australia plate subducts beneath the Sunda block at about 70 mm/yr in a nearly margin-normal direction. The main bathymetric feature off central and eastern Java is the Roo Rise. It bears similarities with the Nazca Ridge off Peru (Hampel et al., 2004), also with many seamounts scattered around it. Roughly between 114°E and 120°E, the Roo Rise is subducting beneath the forearc wedge. To the west, subducting geometrical anomalies are numerous individual seamounts, some of which have created re-entrants on the lower continental slope visible on bathymetric maps of higher resolution than Fig. 9 (Kopp et al., 2006; Krabbenhoeft et al., 2010; Masson et al., 1990). Subducting seamounts have been seismically imaged as far west as ~106.5°E (Kopp et al., 2009). Subduction of the rugged seafloor results in a complex structure of the frontal forearc (Kopp et al., 2006, 2009).

Earthquakes along the Java margin have been limited to the small and moderate magnitude range ($M_w < 7.5$) except in two cases, the 1994 $M_w = 7.8$ and 2006 $M_w = 7.7$ tsunami earthquakes (Fig. 9). Both of these events occurred in the shallow, near-trench region of the subduction zone, similar to the Hikurangi (Fig. 4) and Nicaragua (Fig. 5) tsunami earthquake cases. The lack of very large megathrust earthquakes at Java for the entire era of instrumental seismology has been recently verified by Okal (2012) who re-examined all potential candidates. In contrast, the Sumatra subduction zone to the west (Fig. 7) has produced many great earthquakes including the devastating $M_w = 9.2$ event in 2004. Newcomb and McCann (1987) recognised this contrast long before the 2004 event and thought, on the basis of a correlation of event size and the age and speed of the subducting plate (Ruff and Kanamori, 1983), that it might be related to the eastward increase in the age of the subducting AU plate. The correlation of 1983 no longer holds (Stein and Okal, 2007), so other explanations are needed, including the possibility of the contrast being simply an artefact of the relatively short (~one century) instrumental record. However, one is tempted to notice that the incoming seafloor becomes increasingly more rugged towards the east (Fig. 7), with the smoothest part being the area of the 2004 Sumatra earthquake and roughest part being east Java.

The Java margin produced the most widely cited, and arguably the only, example of a subducting seamount causing a large earthquake. The 1994 $M_w = 7.8$ tsunami earthquake occurred beneath a bathymetric high on the lower slope that had earlier been speculated to have been created by a subducting seamount (Masson et al., 1990). Abercrombie et al. (2001) thus proposed that the seamount caused the 1994 earthquake. However, recent seismic imaging along two survey profiles crossing at the top of this bathymetric high (Fig. 9) showed no evidence for the presence of a subducting seamount or any other significant geometrical irregularity (Shulgin et al., 2011). Therefore, the 1994 earthquake ruptured a relatively smooth part of the generally rugged subduction fault. For the 2006 $M_w = 7.7$ tsunami event, it appears that the rupture began in a smoother portion of the fault, with rupture arresting in an area of a bathymetry high (Bilek and Engdahl, 2007). The nearest seismic profile is 100 km away (Kopp et al., 2009), so it is not clear whether this bathymetry high is related to subducted topography.

There have been limited GPS monitoring and measurements in parts of Java. For westernmost Java, a GPS-based model presented by Hanifa et al. (2013) features a mostly creeping plate interface with a patch of more complete locking (87%). For central and eastern Java, the sparse geodetic data cannot yet constrain the locking/creeping state of the megathrust (Abidin et al., 2009; Salman et al., 2013; C. Kreemer, personal communication, 2013). The working hypothesis based on the low seismicity of the past century is that subduction is primarily aseismic along this margin. Given the large population in Java that could be affected by a great megathrust earthquake and its tsunami, it is critically important to test this hypothesis by expanding geodetic monitoring and carrying out seafloor geodesy.

2.8. Mariana

The Mariana subduction zone (Fig. 10), where the PA plate subducts beneath the PS plate, is traditionally regarded as a textbook example of

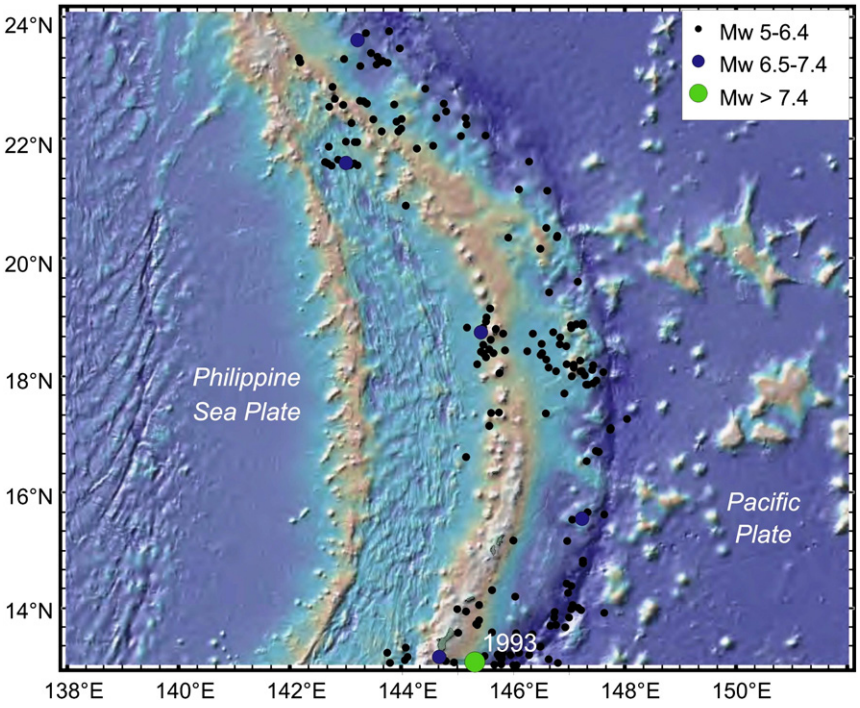

Fig. 10. Seismicity of the Mariana subduction zone, traditionally a textbook example of creeping plate boundary.

aseismic subduction (Uyeda and Kanamori, 1979, and numerous research papers and textbooks). It is also an end-member example of extremely rugged subducting seafloor, featuring numerous seamounts that are approaching the trench, indenting the trench, and being subducted (e.g., Fryer and Smoot, 1985; Oakley et al., 2008; Watts et al., 2010). Morphological signatures of seamounts indenting the frontal forearc are obvious, but they do not seem to create significant topography further arcward (Oakley et al., 2008). Mariana is unique in having another type of seamount, that is, seamounts in the submarine forearc formed by serpentinite mud volcanoes (e.g., Fryer et al., 1985). The serpentinites are formed by the hydration of the forearc mantle that for most part is less than 15 km below the seafloor. The mantle wedge between the overriding crust and the subducting slab is very thin (Oakley et al., 2008) and probably rather thoroughly hydrated by fluids released from the slab, forming low-temperature serpentine species (lizardite and chrysotile) that are weak and buoyant (Wada and Wang, 2009).

It is well known that seismicity along the Marianas Trench is dominantly of small and moderate magnitude, well distributed along the margin. One event in 1993 ($M_w = 7.7$) near Guam is identified as a thrust mechanism event in the GCMT catalogue, although various studies suggest that it occurred within the subducting slab rather than along the megathrust (e.g. Emry et al., 2011). Through analysing earthquake data recorded using a local ocean bottom seismometer network, Emry et al. (2011) identified numerous small earthquakes widely distributed along the plate interface. They reasoned that the interface is creeping while producing seismicity on small seismogenic patches, supporting the traditional view of aseismic subduction. The abundance of weak serpentine minerals should further facilitate creep.

Because the forearc is under water and the trench is very deep, it is technologically impractical at present to use geodetic measurements to constrain the creeping/locking state of the subduction fault. Using campaign GPS measurements on the Mariana island arc during 1992–1999, Kato et al. (2003) demonstrates that, due to back arc spreading, the Mariana arc is moving away from the PS plate at a rate of 16 mm/yr at latitude ~18.75°N increasing southward to 45 mm/yr at ~13.5°N. They thus infer that convergence between the Mariana arc and PA plate increases from 35–45 mm/yr to 55–70 mm/yr over this latitudinal range.

2.9. New Hebrides: a possible counter example

At the roughly north–south oriented New Hebrides Trench, the Australia plate subducts eastward beneath the western North Fiji Basin. By inverting GPS data from Calmant et al. (2003), Power et al. (2012) and Wallace et al. (2012) determined the locking state of the subduction megathrust and simultaneously several other block boundaries in the western North Fuji Basin which undergoes very active and complex internal deformation. Their results show full locking in central New Hebrides where the aseismic D'Entrecasteaux ridge collides into and subducts beneath the New Hebrides island arc but significant creep to the north and south where the subducting seafloor is smoother.

In the north and south of central New Hebrides, GPS data contain no information on margin-normal strain because of the small number of stations and their linear distribution along strike. The inferred creeping state of the megathrust thus depends on, and suffers from ambiguities in, the regional kinematic model and motion of other boundaries. At central New Hebrides, the network configuration allows a strain rate to be estimated, and it indeed shows margin-normal shortening. However, it is well documented (Fisher et al., 1991; Louat and Pelletier, 1989; Meffre and Crawford, 2001) that the D'Entrecasteaux ridge and a similar topographic feature about 10 km to the south, as they collide into the central New Hebrides, cause significant permanent margin-normal shortening as well as uplift of the upper plate. It is to be determined how much of the geodetically observed contractile strain rate in this area reflects this permanent deformation and how much reflects interseismic strain accumulation towards a future great megathrust earthquake.

3. Mechanical issues regarding the subduction of geometrical irregularities

In most of the examples reviewed in the preceding section, very rugged subducting seafloor does not cause strong locking of the subduction fault. Instead, it causes the fault to creep at rates comparable to the subduction rate. These subduction zones are thus poor candidates as producers of great megathrust earthquakes.

In contrast, subduction zones that have produced giant earthquakes tend to have rather smooth incoming seafloor as a result of either no significant topography or a substantial blanket of sediments acting to cover existing topography (Scholl et al., 2011). These areas are also home to the vast majority of great (M = 8 or greater) earthquakes. Using the longer duration USGS/NOAA earthquake catalogue and disregarding the non-subduction zone events contained in there, the largest earthquakes occur along the smoother portions of the subduction zone. Isolating the largest events (M > 9, pink lines in Fig. 1), we see that all of these events occur in smooth regions. Numerous geodetic studies have reported high degrees of locking of large fault patches at these subduction zones at present or prior to a recent giant earthquake: Cascadia (McCaffrey et al., 2013; Wang et al., 2003), Alaska (Suito and Freymueller, 2009), South-Central Chile (Moreno et al., 2011), Sumatra north and south of the IFZ (Chlieh et al., 2008), Japan Trench (Hashimoto et al., 2009b; Loveless and Meade, 2010; Suwa et al., 2006), and southern Kamchatka (Bürgmann et al., 2005).

In this section, we provide a critical review of relevant mechanical concepts about the role of subducting geometrical irregularities, especially the role of subducting seamounts, in controlling megathrust earthquakes. There are many other factors that can affect fault slip behaviour (see Introduction), but we focus on why geometrical irregularities hinder large rupture and cause creep.

3.1. Irregular geometry is not heterogeneous friction

The most common mistake in conceptualising how subducting seamounts or other topographic features affect subduction earthquakes is to regard geometrical irregularities as frictional anomalies regardless of their size. For example, Scholz and Small (1997) proposed that the primary effect of a subducting seamount is to increase stress normal to the fault because of the flexural rigidity of the upper plate, and that the resultant greater shear strength makes the fault patch prone to seismic ruptures of very long recurrence intervals. Here not only the application of the flexure model is implausible (Wang and Bilek, 2011), but also the critically important role of the irregular geometry in resisting shear motion and affecting rupture propagation is ignored. Based on this conceptualization, there are numerical models that literally use a planar fault to study the effect of subducting seamounts on earthquake rupture (Duan, 2012; Honkura et al., 1999; Yang et al., 2012). In these models, a seamount is represented by a patch of the planar fault with locally higher normal stress.

In tribology, the study of interacting solid surfaces in relative motion, asperities are protuberances of typically micrometre scales. They collectively give rise to roughness and are responsible for the phenomenon of friction. At the macroscopic scale of geological concern, friction is usually and reasonably represented by the coefficient of friction μ, although strictly speaking the coefficient may not be an intrinsic property of the interface (Ben-David and Fineberg, 2011). Ignoring cohesion, the frictional strength of the interface is given by

$$\tau = \mu(\sigma_n - p) = \mu(1-\lambda)\sigma_n = \mu\sigma_n' = \mu'\sigma_n \quad (1)$$

where σ_n and p are normal stress and pore fluid pressure (at failure), respectively. The effect of pore fluid pressure is expressed in terms of either the effective normal stress $\sigma_n' = \sigma_n(1-\lambda)$ or an effective coefficient of friction $\mu' = \mu(1-\lambda)$, where $\lambda = p/\sigma_n$ but may take various approximate forms with the most popular one putting the weight of the overlying rock column in the place of σ_n. The variation of the frictional strength with slip or slip rate is referred to as the frictional behaviour of the interface. If the strength decreases with increasing slip or slip rate, the sliding may be unstable, resulting in seismic rupture. Therefore, the frictional behaviour is what is of primary interest in earthquake research (Scholz, 1998, 2002). The friction coefficient can be affected by several factors such as gauge material and temperature, and the effective normal stress is controlled strongly by the pore fluid pressure. Spatial variations in geological, thermal, and hydrological conditions thus give rise to heterogeneous friction.

In geological applications, it is reasonable to scale up the concept of asperities leading to friction. At a regional scale, a shear band of several metres thick may be approximated as a sliding frictional contact, and geometrical irregularities of centimetre scale that cause resistance to shear motion may be considered asperities. However, there must be a limit to this scaling. When the geometrical irregularities are very large, such as subducting seamounts that protrude from the slab surface by 1–3 km or more, they are not asperities causing frictional resistance (Wang and Bilek, 2011). Unlike micro-scale asperities that can be more easily overcome through elastic and plastic deformation, it is much more difficult for a seamount to overcome its geometrical incompatibility with its course of motion. Permanent deformation must occur pervasively in a volume of rocks and cannot be described as frictional sliding. Therefore, friction concepts such as friction coefficient and stable or unstable sliding generally do not apply, although they may apply to individual fractures within the broad zone of damage.

The above view appears to differ from the self-affine fractal description of fault surface topography over wavelengths of many orders of magnitude (Candela et al., 2012; Renard et al., 2013). If viewed at vastly different spatial scales, the fault roughness statistically looks the same up to an appropriate scaling of the amplitudes. If so, a subducting seamount is almost a zoomed-up version of a micro-metre asperity. This apparent disparity deserves future research, but here we contend with pointing out some intriguing differences between the fractal description and subduction faults. (1) The fundamental feature of a fractal is scale invariance, and self-affine fault-surface geometry indicates the lack of any inherent scale length in the responsible geological processes. However, faults do have some important scale lengths. Principal slip zones of earthquakes are of thicknesses of millimetres to centimetres (to be further discussed in Section 3.3), and subduction fault zones are typically a few hundred metres thick (further discussed in Section 3.4.1). This means that the related geological processes are not scale invariant. For example, what happens in a gouge layer of a few millimetres thick that lead to shear instability and seismic slip cannot be the same as deformation in and around large subducting topographic features. (2) Although bathymetry can be described using fractals (e.g., Mareschal, 1989), we do not expect subducting seafloor of all subduction zones to share the same fractal statistics. The very smooth subducting seafloor at Cascadia and the very rugged seafloor at the Marianas are distinctly different, and so will be the subduction faults that they shape. If the Mariana seafloor is similar to a fault surface, then the Cascadia seafloor would have to be considered anomalously smooth, and vice versa.

The exact scale limit for geometrical irregularities to be reasonably approximated as frictional asperities is not yet defined and is probably dependent on the rigidity and yield strength of the rock material involved. Limited research indicates that even at relatively small scales, e.g., with geometrical irregularities of tens of metres in width and centimetres in height, relating geometry to friction is already a non-trivial issue (Chester and Chester, 2000; Sagy and Brodsky, 2009). To understand how results of laboratory friction experiments can be extrapolated to real fault zones, much field and modelling work is needed.

The effect of geometry on fault motion is well recognised in structural geology and earthquake research in land settings (King and Nabelek, 1985; Nielsen and Knopoff, 1998; Saucier et al., 1992; Scholz, 2002; Wesnousky, 1988, 2006; Wibberley et al., 2008). The tendency for confusing irregular geometry with heterogeneous friction in subduction zone research is related to the fact that modern subduction faults cannot be visually inspected. It may result from the unfortunate use of the word asperity to describe different things. As is understood in seismology today, a "seismic asperity" is simply a patch of the fault that has greater slip during an earthquake. When the tribological concept of asperity is inappropriately scaled up to describe large topographic features on the subducting slab, it is often confused with seismic asperity. This is

an example of how a seemingly trivial matter of semantics may cause scientific confusion.

3.2. Mechanical scenarios of seamount subduction

Any change in fault geometry in the slip direction gives rise to incompatibility that resists fault motion, and the resistance is usually larger than the frictional resistance provided by a planar fault area of comparable dimension. Subducting seamounts feature rather extreme geometrical changes. An examination of how a seamount subducts helps to understand the lesser effects of more subdued geometrical changes. Fig. 11 illustrates three different scenarios seen in the literature for how a seamount may overcome its geometrical incompatibility. Here we address the geological process of seamount subduction at timescales of hundreds of thousands of years. It is the geological process that determines structural and stress conditions for seismic rupture and aseismic creep. In Section 3.3, we will discuss how seismic rupture might be envisioned to occur under each of these scenarios.

(1) "Cutting off". One way to overcome the geometrical incompatibility is to shear off a part of or the entire seamount (Fig. 11a) (Cloos, 1992; Cloos and Shreve, 1996). Mechanically, this is not impossible but must be rather difficult to accomplish. Unlike the pyramid shape portrayed in cartoons that are used to illustrate this idea, seamounts are disc-like features with a height to width ratio typically less than 10%. "Decapitating" a seamount means peeling off a coherent large sheet of basalt. If the seamount is a volcanic edifice weakly attached to the oceanic crust along a smooth interface, peeling it off may be accomplishable, but the internal structure of volcanoes is usually too complex to accommodate this mechanism (Watts et al., 2010).

More importantly, as Wang and Bilek (2011) explained, there is little geological evidence in exhumed subduction zone complexes for wholesale decapitation of subducting seamounts. For example, Isozaki et al. (1990) reviewed ~500 studies of accreted oceanic material in Japan with accretion depth up to 30 km. About three quarters of the over 800 observed occurrences of basaltic rocks are fragments of subducting seamounts, but these basalt pieces are smaller than seamounts seen in the western Pacific by one to two orders of magnitude. It appears that seamounts are eroded in pieces on its way down (Ueda, 2005; Wakida, 2012), in a way similar to the peeling off of small slices of normal oceanic crust during subduction (Kimura and Ludden, 1995). Therefore most subducting seamounts are expected to survive to 20–30 km depths or deeper. Wholesale seamount decapitation must be rather rare.

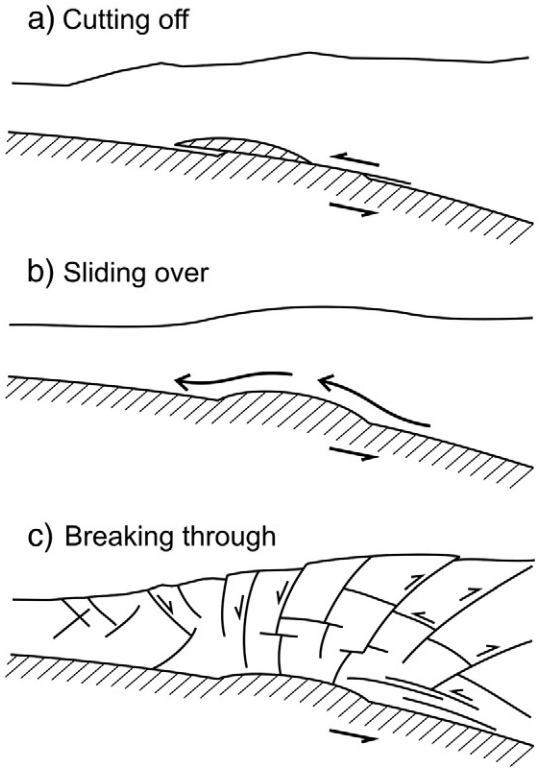

Fig. 11. Scenarios of seamount subduction seen in the literature. (a) "Cutting off": The top part of or the entire seamount is sheared off. (b) "Sliding over": The upper plate frictionally slides over the seamount without severe internal damage. (c) "Breaking through": The seamount forces its way through by severely damaging its surrounding and itself (modified from Wang and Bilek (2011)). We consider (a) unlikely and (b) mechanically impossible. Scenario (c) is supported by field observations and sandbox experiments.

Direct modern evidence for subducting seamounts surviving to large depths is difficult to obtain because of the diminishing resolution of geophysical imaging with increasing depth. However, arcuate burrow scars (re-entrants or "cookie bites") on the lower trench slope and seismic imaging indicate seamount subduction to at least 10 km below sea level in a number of subduction zones (Bell et al., 2010; Kodaira et al., 2000; McIntosh et al., 2007; Mochizuki et al., 2008; von Huene et al., 2000). It is reasonable to infer the presence of seamounts at greater depths. At the Sumatra subduction zone, seismic surveys using a powerful active source and a very long (15 km) streamer yield a clear image of a seamount that has subducted to a depth of 30–40 km (Singh et al., 2011).

There are also examples of indirect inference of seamounts surviving to large depths from vastly different observations. The tectonic uplift of Costa Rica is inferred to be related to seamount subduction to about 20 km depth in the geological past (Fisher et al., 1998). Lineaments in the distribution of non-volcanic seismic tremor now observed at the Nankai subduction zone are inferred to be controlled by scars on the underside of the upper plate marked by subducting seamounts that had travelled at least to the depths of 30–40 km (Ide, 2010). Small earthquakes in the northeast Japan subduction zone above the slab but within the forearc mantle wedge are inferred to be produced by materials of subducting seamounts piled up in the mantle wedge corner (Uchida et al., 2010), implying that these ancient seamounts must have survived to the mantle depth before being scraped off the slab.

Opposite of decapitation, one may also entertain a scenario in which a decollement develops within the overriding plate above the height of the subducting seamount (e.g., Bangs et al., 2006). We do not further explore this scenario in our discussions, because in this situation the seamount has become part of the subducting plate that has a smooth upper surface.

(2) "Sliding over". If a subducting seamount were merely a frictional anomaly, the upper plate material would have to be able to slide along the curved interface with the seamount without damaging itself (Fig. 11b), and principles of friction would apply. The envisioned large elastic deformation of the upper plate would require its material to be very compliant (i.e., extremely low rigidity) and/or very strong (high yield stress). For realistic rigidity and strength in the seismogenic depth range, Wang and Bilek (2011) have shown that the upper plate cannot conform to the shape of a seamount by elastically deforming itself in the way as envisioned by Scholz and Small (1997). As explained in the preceding section, the resistance to seamount subduction is mainly geometrical incompatibility, not a strong frictional contact with the upper plate. Even if the contact could be made frictionless, the geometrical resistance would still be strong.

(3) "Breaking through". In our opinion, the most common way of overcoming the geometrical incompatibility is to permanently (as opposed to elastically) deform the surrounding rocks and, to a lesser degree, the seamount itself (Fig. 11c) (Ballance et al., 1989; Cummins et al., 2002; Wang and Bilek, 2011). At the low-temperature seismogenic depths, the permanent deformation is predominantly in the form of fracturing. Even for accretionary prisms that are often said to consist of soft sediment, mounting geological and seismic evidence demonstrates extensive fracturing and faulting. Fig. 11c (Wang and

Bilek, 2011) illustrates a possible fracture system around the subducting seamount based on the experimental work of Dominguez et al. (1998, 2000), but in a real subduction zone the exact pattern of the fracture distribution must depend on details of the rock rheology of the specific site. For example, the fractures are not necessarily large faults extending to the seafloor.

Along the path of the seamount, the same volume of rock sequentially experiences different modes of failure in response to an evolving stress field. Compressive failure is followed by extensional failure, accompanied with lateral shear. Fracture pattern in the wake of the seamount is thus expected to be very complex. This general pattern of failure is readily verified using continuum numerical models (Baba et al., 2001; Ding and Lin, 2012), although the continuum models cannot simulate the generation and evolution of the fracture system and the resultant heterogeneous stress field. The numerous fractures seen in a recent three-dimensional seismic survey of the frontal forearc of the Costa Rica subduction zone (survey location shown in Fig. 5) are almost undoubtedly the work of a seamount that has passed through the survey area and subducted to a greater depth (Kluesner et al., 2013). The re-entrant marked by this seamount is clearly visible in the seafloor bathymetry. Where subducting seamounts are seismically imaged, the structure is always reported to be very complex (Bangs et al., 2006; Bell et al., 2010; Gulick et al., 2004; Kodaira et al., 2000; McIntosh et al., 2007; Park et al., 2003; Ranero and von Huene, 2000; von Huene et al., 2000). At shallow depths, subducting seamounts usually cause seafloor uplift, and the uplift is accommodated by fracturing, not elastic flexure, of the upper plate.

Subducting seamounts severely deform upper plate rocks and drag their fragments to greater depths. This is recognised to be an important means of subduction erosion (von Huene and Scholl, 1991). The eroded material, mixed with sediments brought down from the trench and rock slices from the seamounts themselves, sometimes are accreted to the upper plate at greater depths. This is considered to be an important process in melange formation (Okamura, 1991; Wakida, 2012).

An assumption used to explain recent observations of largely aseismic subduction of a seamount is that fluid-saturated sediments entrained by the seamount weaken its contact with the overriding plate (Bell et al., 2010; Mochizuki et al., 2008; von Huene, 2008). Depending on the envisioned thickness of the weak material around the seamount, this can be a special version of either "sliding over" or "breaking through". Sliding over does not work as explained above, even if a veneer of weak material could make the sliding contact frictionless. If a thick volume of upper-plate material around the seamount is ductile, it can accommodate the geometrical irregularity by "flowing" around it, that is, the seamount "breaks through" without generating brittle fractures. Singh et al. (2011) proposed that the main reason for the aseismic subduction of the deep seamount they imaged at Sumatra is the ductile behaviour of the overriding mantle wedge. The lack of bathymetric expressions of the many subducting seamounts at Mariana (Oakley et al., 2008) may also be due to the unusual abundance of weak serpentinites in the fault zone and overlying mantle wedge (see Section 2.8).

3.3. Seismic rupture at large geometrical irregularities

In the study of earthquakes in continental settings, there is a general agreement that fault bends and jogs tend to stop large seismic rupture. In contrast, in the subduction zone setting, whether geometrical irregularities such as subducting seamounts tend to generate or stop large earthquakes is a subject of debate. We believe there is much knowledge from continental studies that can be applied to subduction zones.

The abundance of small earthquakes in nature demonstrates that it is not difficult to initiate earthquakes. However, only a very small portion of the initiated events can grow into damaging large ones, as is evident from the Gutenburg–Richter relationship between magnitude and recurrence frequency. It is widely recognised that for small events to develop into large ones, one condition is smooth fault geometry that facilitates rupture propagation. Standard models of the seismogenic portion of faults (Chester and Chester, 1998; Rice and Cocco, 2007; Sibson, 2003; Wibberley et al., 2008) feature a narrow fault core including a primary slip zone (PSZ). The thickness of the PSZ is of the order of a few millimetres to centimetres and does not seem to become larger for larger faults (Shipton et al., 2006; Sibson, 2003). The fault core consists of an ultracataclasite shear zone of centimetres to decimetres thick and, farther out, a gouge zone of up to tens of metres thick. Between this fine-grained fault core and the undamaged country rock, there is a damage zone of tens of metres or much thicker (~10^3 m) consisting of fractured country rocks. Most of the fault motion is accommodated by the fault core, and most of the seismic slip takes place along the PSZ. Geometrical irregularities cause more broadly distributed deformation (Rathbun et al., 2013; Sammis and Steacy, 1994), impede the development of a thin and smooth PSZ, and hence tend to hinder rupture propagation. Therefore, earthquake ruptures often terminate at fault bends, jogs, and stepovers (e.g., King and Nabelek, 1985; Sibson, 1985; Wesnousky, 1988, 2006), although rupture can be arrested for other reasons, such as rate-strengthening frictional behaviour, viscous rock rheology at high temperatures, or stress far below fault strength because of a recent rupture.

Seismic rupture should take place in different ways in the long-term scenarios of Fig. 11. In the "cutting off" scenario (Fig. 11a), the geometrical irregularity is gone. What might affect rupture initiation and propagation can only be material controlled frictional properties (Cloos, 1992), so this scenario is not further discussed. As we explained in Section 3.2, this must be a very rare scenario in nature. In the "sliding over" scenario (Fig. 11b), it is the curvature change of a single fault that may affect the rupture process. Although this scenario is impossible as a long-term geological process as discussed in Section 3.2, it must be considered in studying seismic rupture. For the "breaking through" scenario (Fig. 11c), the effect of curvature change also needs to be considered, but the structural and stress heterogeneities of the fracture system generated by the subducting seamount are more important.

Theoretical and modelling studies show that if a change in fault curvature is the only effect considered, applicable to the "sliding over" scenario (Fig. 11b), the curvature change may hinder but not fully stop rupture propagation. This is because elastic deformation may accommodate the small geometrical incompatibility induced by metres to tens of metres of slip in a few earthquakes. Some of the fault geometries considered in various modelling studies are shown in Fig. 12.

In the 3D elastic model of Oglesby and Archuleta (2003), a thrust fault has a sudden downdip increase in dip (Fig. 12a). In three

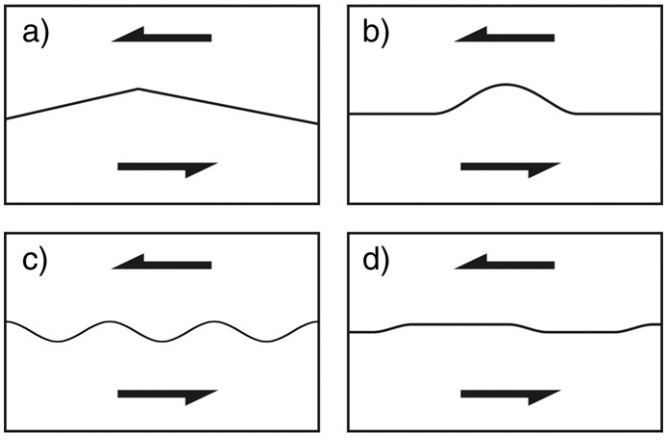

Fig. 12. Various fault geometry used to model the effects of geometrical irregularities on earthquake rupture or other small-displacement fault motion. (a) A kink in the slip direction (e.g., Oglesby and Archuleta, 2003). (b) A seamount (or ridge) in smooth frictional contact with an intact upper plate (e.g., Baba et al., 2001). (c) Wavy fault (e.g., Ritz and Pollard, 2012). (d) Restraining and releasing bends (Nielsen and Knopoff, 1998).

consecutive earthquakes, a rupture initiated downdip of the kink has no difficulty in dynamically propagating updip and over the kink, although slip distributions are different between these events. Oglesby and Archuleta (2003) point out that if many more earthquakes were modelled, the complex stress field around the kink as a result of large cumulative slip might stop rupture propagation. In fact, any dip slip gives rise to a stress singularity at this kink that would cause yielding if the material were not assumed to be purely elastic (Andrews, 1989), but for small slip such as in a few earthquakes, the potential area of yielding is very small such that the effect can be largely ignored.

Yang et al. (2013) used a two-dimensional (2D) dynamic model to examine under what condition a subducting seamount could stop the propagation of a rupture initiated further downdip. This model has no geometrically induced stress singularity because the fault curvature changes gradually (Fig. 12b), but the model is similar to that of Oglesby and Archuleta (2003) in that only a small slip is considered. Yang et al. (2013) demonstrate that, in a single earthquake, the change in fault curvature alone can stop the rupture unless the effective normal stress assigned to the seamount portion of the fault is very small.

Various static models of small slip have also been used to investigate the effect of geometrical irregularities. For example, Baba et al. (2001) considered a static slip model for a seamount structure similar to that of Yang et al. (2013) (Fig. 12b), and Saucier et al. (1992), Ritz and Pollard (2012), and Marshall and Morris (2012) modelled the stress field around a fault that has a wavy shape (Fig. 12c). Because of the small slip, these models are similar to models of single earthquake rupture; it is not very important whether the model is dynamic or static (i.e., including or excluding the inertia force and hence seismic waves). Even if fault opening is not allowed, elastic deformation of the medium can resolve the small space problem caused by the slip. These models all show that the undulating fault topography does not prevent slip but larger amplitude of the topography makes the slip increasingly difficult.

Although small-slip models yield insights into how changes in fault curvature in the slip direction may affect seismic slip, they are not applicable to subducting topographic reliefs. A subduction fault must slip tens of kilometres to deliver a topographic anomaly to 10–20 km depths, and the rock around the anomaly is severely damaged and deformed (Fig. 11c). In this situation, seismic rupture, if any, does not occur along a curved interface between intact upper and lower plates but along slip planes developed in a fractured and sheared rock volume.

The question of how cumulative large slip exacerbates the effect of geometrical irregularities on seismic rupture was partially addressed by Nielsen and Knopoff (1998). In their 2D model, geometrical barriers are restraining and releasing bends of a strike-slip fault (Fig. 12d). After many earthquakes, the cumulative large slip causes large stress at these barriers. In real Earth the stress would be limited by rock strength, and off-fault fracturing and diffusive deformation would relieve the stress. Nielsen and Knopoff (1998) did not directly model the structural and geometrical changes in this "breaking through" process but only addressed the resultant stress relief. By parameterizing the stress relief as a process of viscoelastic relaxation and with a certain choice of viscosity values, Nielsen and Knopoff (1998) showed that the geometrical barriers would usually stop seismic slip but occasionally rupture together with neighbouring planar segments to result in a large earthquake.

The internal structure of the fault zone due to long-term deformation around geometrical irregularities determines how the fault moves in and between large earthquakes, but the complexity of this deformation process presents great challenges for modelling studies. The work of Nielsen and Knopoff (1998) is a major improvement over small-slip models, but it is still quite different from what we may expect from geological reality. Multi-scale brittle failure of crustal rocks around geometrical irregularities is expected to give rise to locally heterogeneous structures and stresses that will affect rupture initiation and propagation. When the failure process is modelled using viscoelastic relaxation or other types of continuum flow, both the structure and stress fields become much smoother. Discrete element methods have the potential of addressing both long-term multi-scale brittle deformation and seismic rupture (e.g., Fournier and Morgan, 2012), but their capability of dealing with comminution is still limited. At present, the link between long-term structural evolution and seismic behaviour around geometrical irregularities is made largely by inferences and reasoning (e.g., King and Nabelek, 1985; Wang and Bilek, 2011).

3.4. Mechanisms of fault creep in subduction zones

Geodetically inferred creep of subduction faults is very widely reported. It is rare to see published megathrust locking models without subconvergence creep ("partial coupling", "partial locking") in parts of the fault in the low-temperature seismogenic depth range, although the creep is usually not as predominant as in Figs. 2 through 10. The predominant creep behaviour for the majority of subduction zones as inferred from moment release by subduction earthquakes (e.g., Pacheco et al., 1993) is subject to large errors because instrumental seismic records are too short to capture many of the largest earthquakes, but it must be telling some truth for margins where modern geodetic observations also indicate creep. Fault creep is reported also for continental settings but not as widely as for subduction zones (Scholz, 2002), the best documented case being the ~120 km long creeping segment of the San Andreas Fault (SAF) (Titus et al., 2006).

We emphasise that the megathrust creep being discussed here occurs at rather low temperatures. Fagereng and Ellis (2009) and Wallace et al. (2012) propose that in some subduction zones such as Kyushu (Fig. 2), northern Hikurangi (Fig. 4), and possibly New Hebrides (but see Section 2.9 about ambiguity in geodetically determined creep), megathrust creep can be thermally activated (dislocation creep) even at these low temperatures. They reason that if the fault is frictionally very strong due to low pore fluid pressure (see Eq. (1)), the downdip transition from frictional sliding to thermally activated viscous creep occurs at a very shallow depth (such as 15–20 km), so that most of the fault should undergo viscous creep except the shallowest portion. Despite its appealing simplicity, we do not think it can be a common mechanism. For example, at Kyushu and northern Hikurangi, frictional/shear heating calculation using realistic fault geometry and constrained by forearc heat flow observations does not suggest a frictionally strong megathrust and a consequent shallow transition to viscous creep (Wada and Wang, 2009). In northern Hikurangi (Section 2.3), frequent occurrence of slow slip events at rather shallow depths, rarely exceeding 15 km and possibly as shallow as the trench (Wallace and Beavan, 2010), does not suggest a strong shallow fault. In Kyushu (Section 2.1), the occurrence of moderate-size megathrust earthquakes to 30–40 km depths (Yamamoto et al., 2013) does not support thermally activated creep.

3.4.1. Creeping as a result of broad deformation

The most commonly discussed fault creep behaviour is for relatively smooth faults and is explained by various proposed or laboratory observed mechanisms. For example, the SAF creep is attributed to the presence of weak minerals such as talc (Moore and Rymer, 2007) and saponite (Lockner et al., 2011) in the fault gauge or to pressure solution creep of fault zone material (Gratier et al., 2013a). Modelled as a frictional contact, smooth-fault creep is a consequence of rate-strengthening behaviour, but a rate-strengthening fault patch may exhibit dramatic weakening to participate in a seismic rupture if driven to slip at a sufficiently high rate (Noda and Lapusta, 2013). Even without high-rate weakening, seismic slip can propagate into or through a rate-strengthening segment depending on the size of the segment and its degree of strengthening (Boulton et al., 2012; Hu and Wang, 2008; Kozdon and Dunham, 2013).

Exhumed ancient subduction zones show subduction faults to be broad zones of complex internal structure, with strong evidence for

cataclastic flow and pressure solution creep as well as seismic slip (Vannucchi et al., 2006; Bachmann et al., 2009; Meneghini and Moore, 2007; Fagereng and Sibson, 2010; Kimura et al., 2012). By synthesising observations from ancient and active subduction zones, Rowe et al. (2013) show that, down to ~15 km depth, subduction faults are melange zones of several hundred metres thickness including highly sheared strands of tens of metres thickness which may host discrete seismic slip zones of millimetres to 20 cm thickness. This is pretty much like the structure of large strike-slip faults observed on land (Faulkner et al., 2010). Kitamura and Kimura (2012) and Rowe et al. (2013) explain that the fabrics of the broad fault zone and the shear strands indicate significant creep motion that can be fast enough to accommodate postseismic slip and episodic slow slip events. Cataclasis and pressure solution are predominant creep mechanisms. The subducting plate releases fluids either through pore collapse or metamorphic dehydration of hydrous minerals, and the abundance of fluids should facilitate pressure solution creep (Gratier et al., 2013b).

To investigate why irregular geometry leads to creep, we consider the subduction of extreme roughness such as seamounts in the context of the internal structure of subduction fault zones. As discussed in Section 3.2, the most likely mode of seamount subduction is "breaking through" (Fig. 11c). Ductile "breaking through" discussed at the end of Section 3.2 may happen at very shallow depths beneath a frontal prism that consists of unconsolidated sediments and rock debris. This may also happen when the seamount is in contact with hydrated mantle wedge or where high temperature allows thermally activated rock creep. For seismogenic depths where rocks generally exhibit brittle behaviour, "breaking through" is likely accomplished by fracturing.

Wang and Bilek (2011) reasoned that the evolving fracture network around the seamount creates both structural and stress heterogeneities. At any time, some fractures in the system are at or near failure while other fractures are still far from failure. Failure of individual fractures tends to be limited in dimension because of the difficulty of rupture propagation in very heterogeneous structural and stress environments. As a result of alternating failure of various parts, the system must be deforming very frequently or more or less constantly. However, earthquakes around subducting seamounts and in areas of very rugged subducting seafloor tend to be small and, although numerous, far from enough to accommodate plate subduction. The key question is why the evolution of the fracture system is predominantly aseismic. We speculate there are two primary reasons. First, the fracturing process must be accompanied with brecciation and comminution and resultant cataclastic flow. The anomalously high b-values of ~2, as compared to the global average of ~1, in the seamount subduction area of southernmost Nicoya, Costa Rica (Fig. 5), indicates a much larger than usual number of small earthquakes (Ghosh et al., 2008). Extrapolating this trend towards very low magnitudes may suggest the presence of massive amounts of brittle failure events that are too small to be recorded as earthquakes even with near-field seismometers. Second, the highly fractured rocks allow a wide distribution of fluids, so that pressure solution creep is pervasively active over a large volume around the seamount, causing creep along many block and grain boundaries in this system.

3.4.2. Strength of creeping faults

An intriguing subject is the strength of creeping faults. Creeping faults are commonly said to be weak, and seismogenic faults are said to be strong. This may be true for smooth faults, that is, a locked rate-weakening fault patch may sustain higher shear stress than a rate-strengthening creeping patch (already at failure). This may not be true for a very rough fault for which much of the resistance against creep is geometrical incompatibility. As discussed above, "breaking through" the incompatibility is not a frictional process. Using subducting seamounts as an example, three views of the strength of locked and creeping faults can be summarised in Fig. 13. In the "breaking through" model, if the subduction of a seamount requires fracturing its surrounding, the geometrical resistance against its creep is generally stronger than the locking stress of a smooth fault (Fig. 13a) (Wang and Bilek, 2011). If the upper plate is soft enough to allow ductile "breaking through", the resistance to creep can be lower than the locking stress of a smooth fault (Fig. 13b) (Mochizuki et al., 2008). Fig. 13c shows the situation if the seamount is incorrectly conceptualised as a seismogenic frictional anomaly of no structural effects.

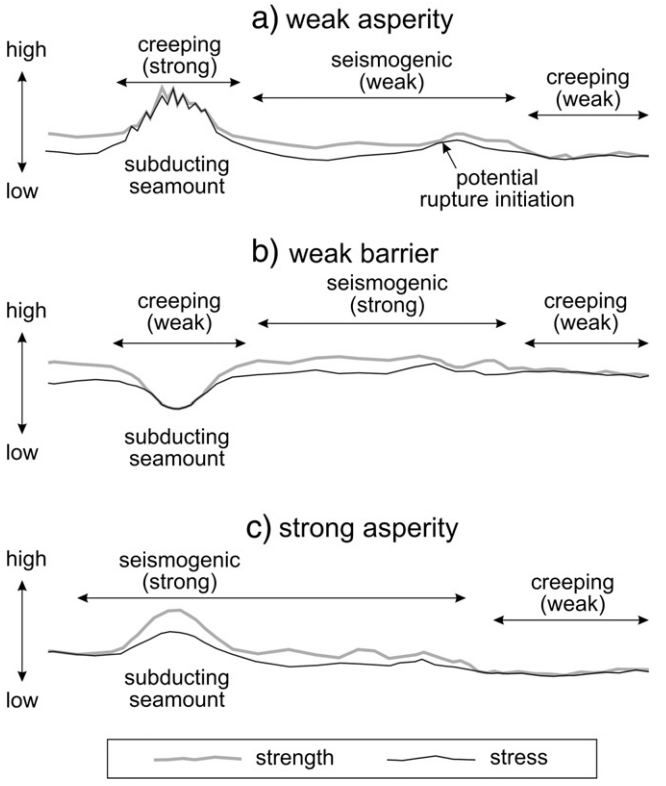

Fig. 13. Cartoon illustration of fault strength and stress in different conceptual models involving a subducting seamount. (a) The seamount creeps against strong resistance; smoother and weaker fault areas allow rupture propagation (Wang and Bilek, 2011). Jaggedness of the stress/strength curves in the seamount area is meant to emphasize structural and stress complexity associated with a fracture system as opposed to a single interface. (b) The seamount creeps against little resistance; smoother and stronger fault areas allow rupture propagation (Mochizuki et al., 2008). (c) The seamount is only a frictionally strong patch of the fault.

3.4.3. Spatial and temporal variations of creep

Creep of smooth faults often produces small repeating earthquakes, which is understood to be repeated rupture of rate-weakening patches embedded in an otherwise rate-strengthening fault (e.g., Chen and Lapusta, 2009). Rough-fault creep is seen to exhibit a greater variety of spatial and temporal patterns. Interspersed rough and smooth areas of a rugged subducting seafloor result in a mixture of creep and moderate size earthquakes. If a narrow rough zone is situated in the stress shadow of two large seismogenic patches, such as the long-term rupture barrier between the 2004 and 2005 great Sumatra earthquakes (Meltzner et al., 2012), it may not exhibit much creep. Instead, it may partially slip during earthquakes while resisting the rupture generated by its seismic neighbour.

Temporally, creep may be accommodated in slip pulses by slow slip events, as observed off northern Hikurangi (see Section 2.3). Given the heterogeneous structural, stress, and pore fluid pressure conditions produced by the subduction of rugged seafloor, it is reasonable to infer that transient slip events may exhibit a wide range of slip rates. Some may be too slow to be detected with the present resolution of geodetic observations. Some smoother patches may occasionally slip fast enough to produce tsunami earthquakes as reported for northern Hikurangi

(Section 2.3), Nicaragua (Section 2.4), and Java (Section 2.7). In a way, small and medium regular earthquakes are simply the fastest version of transient slip events. We anticipate that future high-resolution, near-field seafloor or borehole strain monitoring will further demonstrate the wide variety of slip events.

3.4.4. Sub-convergence creep and large earthquakes

If a megathrust is creeping at a rate slower than plate subduction, it is accumulating a slip deficit. For seismic and tsunami hazard assessments, it is an important question how this deficit will be recovered. If the observed creeping ratio is 70%, is the rest of the 30% being stored as elastic strain energy only to be released by a future great earthquake? If so, creeping would only serve to lengthen the recurrence interval of great earthquakes. Here we assume sub-convergence creep truly happens over large segments of subduction faults, although we recognise that some of it must be artefacts of poor geodetic resolution.

For a relatively smooth fault, interseismic creep may occur because of aseismic shear deformation of wall rocks adjacent to a locked seismic slip zone (Kitamura and Kimura, 2012; Rowe et al., 2013). But subduction of very rough seafloor will destroy such layered structure of the fault zone. If creeping of very rough faults is accommodated by fracturing and permanent deformation in a broad zone of damage, the resultant heterogeneous structure and stress field should be very unfavourable for rupture propagation and hence unlikely to allow very large earthquakes. Then the slip deficit accrued in sub-convergence creep may have to be recovered by pulses of super-convergence creep of various timescales as discussed in Section 3.4.3, as well as many small and medium earthquakes. The spontaneous slip transients observed at northern Hikurangi (Section 2.3) are high-rate examples of super-convergence creep pulses, and they indeed seem to recover a large fraction of the slip deficit if the poor-resolution near-trench results in Fig. 4 are ignored (Wallace and Beavan, 2010).

The spatial variations of fault creep behaviour discussed in Section 3.4.3 may cause sub-convergence creep. Because of stress shadowing, there is a zone of no or low slip around any locked patch (Hetland and Simons, 2010; Wang, 2007). Therefore, the overall slip deficit of a fault segment with interspersed seismogenic and creeping patches can be much larger than predicted from the total size of the seismogenic patches. Stress-shadowed creep zones usually catch up with plate subduction by having fast afterslip following the rupture of neighbouring seismogenic patches. Such seismically triggered slip transients are as effective as the Hikurangi-type spontaneous slip transients in recovering slip deficits.

The question regarding slip deficit of sub-convergence creep cannot be fully addressed until the creeping mechanism is fully understood. Although physical reasoning makes creeping subduction faults, especially those with very rugged subducting seafloor, poor candidates as potential hosts of great or giant earthquakes, much observational and theoretical research is needed to clarify the issue. The most direct observational method is near-trench seafloor monitoring to constrain displacement and strain and hence fault creeping rates and their changes with time.

4. The role of subducting seamounts in the M = 9 Tohoku earthquake

All instrumentally recorded giant events have occurred at subduction zones with a smooth subducting seafloor (Fig. 1). Extremely rugged subducting seafloor leads to fault creep at significant rates without producing very large megathrust earthquakes (Figs. 2–10). At odds with these observations are proposals that a subducting seamount may have been responsible for producing the 2011 Tohoku earthquake. The Tohoku earthquake is the best instrumentally observed giant megathrust event and thus provides opportunities to advance our understanding of geological control of subduction earthquakes worldwide. It is therefore worth the effort to re-evaluate the role of subducting seamounts in this event.

We are not aware of any geophysical imaging that shows the presence of a subducting seamount in the main rupture area of the Tohoku earthquake. Neither does the extrapolation of seamount chains on the incoming Pacific plate (Fig. 14) suggest the potential presence of a subducting seamount of significant size in this area. The idea that a subducting seamount may have caused this earthquake is based indirectly on two observations: (1) Seismic tomography shows an area of high P-wave speed (V_p) in the main rupture area between low-V_p areas to the north and south (Zhao et al., 2011), and (2) stress drop is locally as high as 40 MPa in a small part of the epicentral area (Kumagai et al., 2012).

The V_p distribution displayed by Zhao et al. (2011) is from the tomographic model of Huang et al. (2011) which has a lateral grid spacing of 30 km and vertical spacing of 10–15 km in the forearc area. This grid resolution would not allow the imaging of subducting seamounts or other topographic features. The high- and low-V_p anomalies in the 3D tomographic image have vertical dimensions of tens of kilometres as is expected from the grid resolution (see Fig. 2b through e of Zhao et al., 2011). The map-view V_p distribution presented by Zhao et al. (2011) shows the bottom part of these anomalies. It represents wave speed variations in the upper plate, not in the megathrust fault zone. It is much more reasonable to explain these variations in terms of rock properties or fluid contents (Huang et al., 2011; Sibson, 2013) than in terms of subducting topography.

Higher stress drop (40 MPa) in a small fault patch was used to argue for the presence of a subducting seamount (Kumagai et al., 2012). It was envisioned that the small area of large stress drop was more strongly locked before the earthquake because of the seamount. Large spatial variations of fault strength should be common in subduction zones, but higher strength does not always need geometrical anomalies. This can be shown with a back-of-the-envelope calculation using Eq. (1). If other parameters stay the same, tripling the shear strength (e.g., from 30 MPa to 90 MPa) in one patch of a smooth fault only requires lowering λ from 0.9 to 0.7, a rather mundane variation in the pore fluid pressure field in natural subduction zones (Saffer and Tobin, 2011; Sibson, 2013). Having a local stress drop of 40 MPa on such a higher-strength smooth patch is not surprising. Above all, as explained in Section 3.1, if a geometrical irregularity is indeed involved, it should not be confused with a patch of anomalous frictional strength.

Therefore, the argument for a subducting seamount causing the Tohoku earthquake is very weak. On the contrary, there are stronger arguments that subducting seamounts stopped the earthquake. This is obvious at the southern terminus of the main rupture zone (Fig. 14) where the Joban seamount chain is subducting, including the half-subducted Daiichi–Kashima seamount (Nishizawa et al., 2009) and a well imaged fully subducted seamount that is creeping (Mochizuki et al., 2008). All published rupture models for the Tohoku earthquake, four of which are shown in Fig. 14, indicate that rupture propagation stopped in this area, consistent with the notion that extremely rugged subducting seafloor tends to stop large earthquakes. Farther south, the lower plate becomes the PS plate (Fig. 14), but this is unlikely the reason for the rupture arrest because the coseismic slip, about 50 m in the epicentral area, diminished to rather small values or fully stopped a long way before this change.

Most geodetic locking models for the Japan Trench published prior to the Tohoku earthquake did not include the southern seamount subduction area. The two models that did (Loveless and Meade, 2010; Suwa et al., 2006) both showed significant megathrust creep in this area, consistent with patterns seen in other subduction zones of extremely rugged incoming seafloor (Figs. 2 through 10). Similar to the locking/creeping models reviewed in Section 2, all the Tohoku locking models poorly define the location of locked patches in the margin-normal direction because all the geodetic stations were on land and because viscoelastic rheology was not or insufficiently accounted for (Wang et al., 2012), but along-strike variations in the locking/creeping state of the megathrust are robust results.

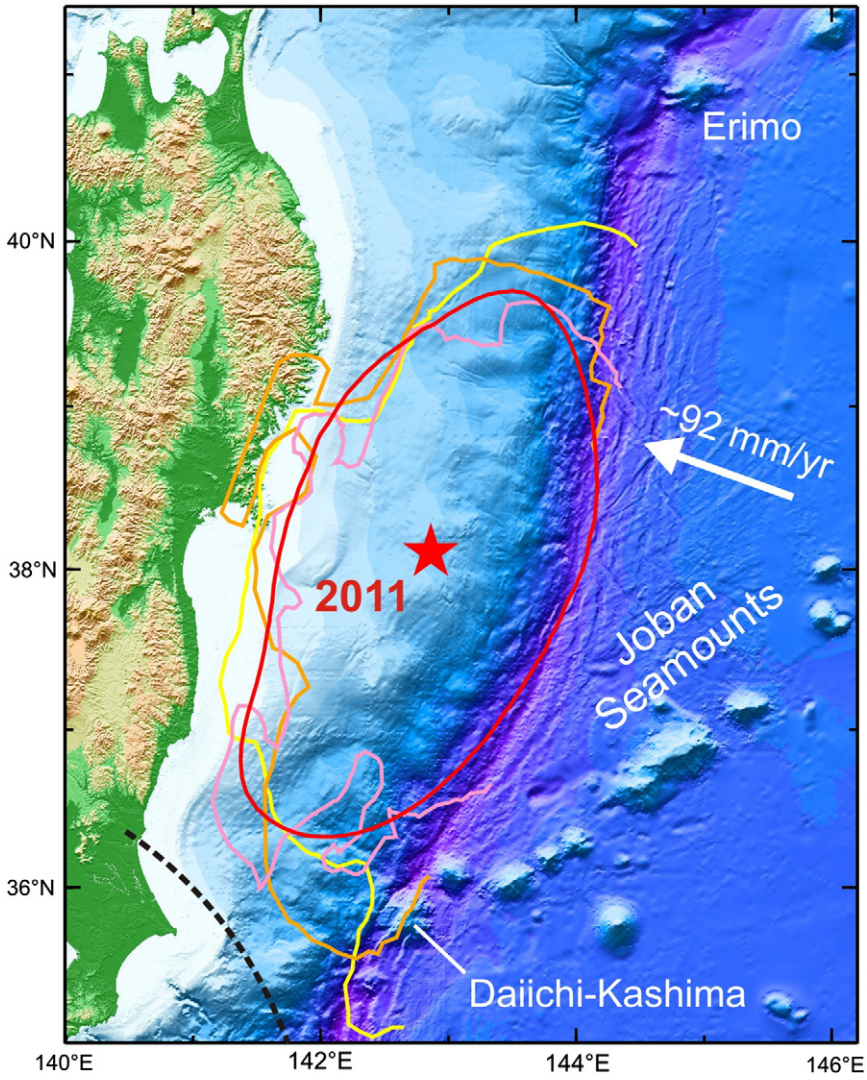

Fig. 14. Map of Japan Trench. Star indicates epicentre of the 2011 Tohoku earthquake determined by the Japan Meteorological Agency. Colour lines are 2-m contours of coseismic slip models that outline the main rupture area: yellow — Lee et al. (2011), pink — Shao et al. (2012), orange — Wei et al. (2012), and red — Wang (2011). The maximum slip in these models is about 45–60 m in the epicentral area. Wang (2011) inverted only GPS data but using real megathrust geometry. The other workers jointly inverted seismic and GPS data but using a planar or piecewise planar fault. Seafloor GPS data were used in all these models. Southward rupture propagation stopped in the area of the subduction of the Joban seamount chain. Incoming seafloor off the main rupture area is rather smooth with small-scale roughness due to horst–graben structure. Black dashed line shows the northern limit of the subducting PS plate defined by Uchida et al. (2009).

The northern termination of the Tohoku rupture is also proposed to be associated with very rugged subducting seafloor (e.g., Kundu et al., 2012), although the association is not as convincing as in the south. Several seamounts are scattered off northernmost Honshu (Fig. 14), including the Erimo seamount that has just begun diving into the subduction zone (Nishizawa et al., 2009). It is not far-fetched to speculate the presence of subducting seamounts in that area. Whatever the reason, the northern area of the megathrust exhibits greater heterogeneity and had ruptured in many medium to large earthquakes prior to 2011 (Yamanaka and Kikuchi, 2004).

In contrast, the seafloor off the main rupture area of the Tohoku earthquake is rather featureless (Fig. 14), and the plate interface is expected to be smooth. Seismic imaging of the shallow (<15 km) part of the megathrust zone indeed shows a very smooth fault (Kodaira et al., 2012; Tsuru et al., 2002). However, the shortage of trench sediment and the well observed and documented horst–graben structure (Tsuru et al., 2002) make the subducting seafloor less smooth than those at Cascadia, Alaska, South Chile, and northern Sumatra (Fig. 1). The horst–graben structure should result in subduction of sediment sections of variable thicknesses, ranging from zero on tall horsts to a couple of hundred metres in deep grabens. This should give rise to multi-scale variations in material properties and pore fluid pressure along the megathrust fault and may be responsible for the wide variety of megathrust behaviour including creep, repeating earthquakes, small and large earthquakes, and giant earthquakes. The cartoon picture of nested mosaics of seismogenic patches seen in Wang (2007) and Uchida and Matsuzawa (2011) seems to apply to the smooth part of the Tohoku megathrust quite well.

5. Conclusions and future directions

Among the many factors controlling the size and recurrence of great subduction earthquakes, subducting seafloor topography is one of first-order importance. Opinions on the role of large subducting geometrical features range from causing large earthquakes to causing aseismic creep. In this article, we have reviewed seismicity and geodetically determined megathrust creeping states for subduction zones or segments where extremely rugged seafloor is being subducted. Our findings can be summarised as the following conclusions.

1. There is strong geodetic evidence that subduction of very rugged seafloor causes aseismic creep of the resultant rough faults. Although

creeping is seen for both smooth and rough faults, there is lack of evidence for rough faults to be more "strongly locked." Creeping faults are unlikely to host great and giant earthquakes.

2. Two examples, the Nazca Ridge and the Investigator Fracture Zone, demonstrate that even a solitary topographic feature between smooth areas of seafloor can cause fault creep, if they are too wide to be fully stopped by stress shadows of neighbouring locked segments.
3. Subducting seamounts are end-member examples of geometrical irregularities. In our review, we have found no evidence for any subducting seamount to have caused any large earthquake, although there are proposed connections between subducting seamounts and small and medium size earthquakes. When a large rupture does manage to propagate into or through an area of seamount subduction, it tends to slow down in that area.
4. In the $M_w = 9$ March 2011 Tohoku earthquake, the southern termination of the rupture occurred in an area of seamount subduction, and the northern termination occurred in an area of complex history of seismic behaviour. The main rupture area features rather smooth incoming seafloor.

We have also provided a critique of physical concepts regarding how geometrical irregularities affect seismogenic behaviour of faults, especially subduction faults. Results of many observational and theoretical studies conducted in continental settings are applicable to subduction zones. Based on these discussions as well as the review of geodetic and seismic observations, we think that much can be learned by pursuing research in the following directions.

1. For fault creep, there is a need to distinguish between frictional stable sliding along a smooth fault and distributed shear deformation of a fault zone. It is important to understand the scale limit for geometrical irregularities to be meaningfully considered as frictional asperities. Between the micrometre-scale geometrical asperities that are responsible for friction and the kilometre-scale subducting seamounts, there is a wide range of mechanical processes to be theoretically and experimentally explored. In this regard, development of laboratory and modelling methods that can simultaneously handle fracturing, comminution, granular flow, pressure solution creep, and slip localization will be very useful.
2. Most geophysical imaging of subduction faults is along 2D transects and for relatively shallow depths (<15 km). 3D seismic imaging of fault zones that are creeping at shallow depths and wide applications of deep penetrating high-resolution geophysical imaging methods will greatly improve our knowledge of the geometry and internal structure of subduction fault zones.
3. Scientific drilling of (shallow) subduction megathrusts and field studies of exhumed ancient subduction zones should go much beyond understanding seismic slip. Creeping, including slip transients, is an important mode of subduction, and there is a general need to constrain its spatial and temporal characteristics at borehole and outcrop scales, with the help of laboratory studies of rock rheology and deformation fabrics. There is special need to study how subducting geometrical features cause creep in a relatively low-temperature but fluid-rich environment.
4. Currently all regional locking/creeping models for subduction faults severely lack near-trench resolution. There is urgent need to conduct seafloor displacement and strain monitoring to constrain temporal and spatial variations of creep (including slip transients). Technology developments are making seafloor geodesy more affordable. Wide applications of seafloor geodesy to subduction zones promise breakthrough discoveries over the next decade.
5. Although not fully explored in this review, there seems to be a general tendency that very large subduction earthquakes occur in areas of smooth subducting seafloor but are absent or rare in areas of very rugged subducting seafloor. For both earthquake physics and hazard assessment, it is important to investigate this tendency, including reasons for exceptions if any and its interplay with other processes that also affect earthquake size and recurrence.

Acknowledgements

We thank L. Wallace, M. Chlieh, Y.-J. Hsu, P. LeFemina, and L. Feng for making available digital values of the creeping ratios displayed in Figs. 2 through 8. L. Wallace, T. Candela, F. Corbi, and F. Funiciello provided valuable suggestions upon reading an earlier version of the manuscript. This is Geological Survey of Canada contribution 20130284.

References

Abercrombie, R.E., Antolik, M., Felzer, K., Ekstrom, G., 2001. The 1994 Java tsunami earthquake: slip over a subducting seamount. J. Geophys. Res. 106, 6595–6607.
Abidin, H.Z., Andreas, H., Kato, T., Ito, T., Meilano, I., Kimata, F., Natawidjaja, D.H., Harjono, H., 2009. Crustal deformation studies in Java (Indonesia) using GPS. J. Earthq. Tsunami 3, 77–88. http://dx.doi.org/10.1142/S1793431109000445.
Ando, M., 1975. Source mechanisms and tectonic significance of historical earthquakes along the Nankai trough. Tectonophysics 27, 119–140.
Andrews, D.J., 1989. Mechanics of fault junctions. J. Geophys. Res. 94, 9389–9397.
Baba, T., Hori, T., Hirano, S., Cummins, P., Park, J.-P., Kameyama, M., Kaneda, Y., 2001. Deformation of a seamount subducting beneath an accretionary prism: constraints from numerical simulation. Geophys. Res. Lett. vol. 28, 1827–1830.
Bachmann, R., Oncken, O., Glodny, J., Seifert, W., Georgieva, V., Sudo, M., 2009. Exposed plate interface in the European Alps reveals fabric styles and gradients related to an ancient seismogenic coupling zone. J. Geophys. Res. 114, B05402. http://dx.doi.org/10.1029/2008JB005927.
Ballance, P.F., Scholl, D.W., Vallier, T.L., Stevenson, A.J., Ryan, H., Herzer, R.H., 1989. Subduction of a Late Cretaceous Seamount of the Louisville Ridge at the Tonga Trench: a model of normal and accelerated tectonic erosion. Tectonics 8 (5), 953–962. http://dx.doi.org/10.1029/TC008i005p00953.
Bangs, N.L.B., Gulick, S.P.S., Shipley, T.H., 2006. Seamount subduction erosion in the Nankai Trough and its potential impact on the seismogenic zone. Geology 34, 701–704.
Barker, D.H.N., Sutherland, R., Henrys, S., Bannister, S., 2009. Geometry of the Hikurangi subduction thrust and upper plate, North Island, New Zealand. Geochem. Geophys. Geosyst. 10, Q02007. http://dx.doi.org/10.1029/2008GC002153.
Bell, R., Sutherland, R., Barker, D.H.N., Henrys, S., Bannister, S., Wallace, L., Beavan, J., 2010. Seismic reflection character of the Hikurangi subduction interface, New Zealand, in the region of repeated Gisborne slow slip events. Geophys. J. Int. 180, 34–48.
Ben-David, O., Fineberg, J., 2011. Static friction coefficient is not a material constant. Phys. Rev. Lett. 106, 254301. http://dx.doi.org/10.1103/PhysRevLett.106.25403.
Bilek, S.L., 2007. Influence of subducting topography on earthquake rupture. In: Dixon, T., Moore, C. (Eds.), The Seismogenic Zone of Subduction Thrust Faults. Columbia University Press, pp. 123–146.
Bilek, S.L., 2010. Seismicity along the South American subduction zone: review of large earthquakes, tsunamis, and subduction zone complexity. Tectonophysics 495, 2–14. http://dx.doi.org/10.1016/j.tecto.2009.02.037.
Bilek, S.L., Engdahl, E.R., 2007. Rupture characterization and aftershock relocations for the 1994 and 2006 tsunami earthquakes in the Java subduction zone. Geophys. Res. Lett. vol. 34. http://dx.doi.org/10.1029/2007GL031357.
Bilek, S.L., Schwartz, S.Y., DeShon, H.R., 2003. Control of seafloor roughness on earthquake rupture behaviour. Geology 31, 455–458.
Bird, P., 2003. An updated digital model of plate boundaries. Geochem. Geophys. Geosyst. 4 (3), 1027. http://dx.doi.org/10.1029/2001GC000252.
Bock, Y., Prawirodirdjo, L., Genrich, J.F., Stevens, C.W., McCaffrey, R., Subarya, C., Puntodewo, S.S.O., Calais, E., 2003. Crustal motion in Indonesia from global positioning system measurements. J. Geophys. Res. 108 (B8), 2367. http://dx.doi.org/10.1029/2001JB000324.
Boulton, C., Carpenter, B.M., Toy, V., Marone, C., 2012. Physical properties of surface outcrop cataclastic fault rocks, Alpine Fault, New Zealand. Geochem. Geophys. Geosyst. 13, Q01018. http://dx.doi.org/10.1029/2011GC003872.
Briggs, R.W., et al., 2006. Deformation and slip along the Sunda megathrust during the great Nias–Simeulue earthquake of March 2005. Science 311, 1897–1901. http://dx.doi.org/10.1126/science.1122602.
Bürgmann, R., Kogan, M.G., Steblov, G.M., Hilley, G., Levin, V.E., Apel, E., 2005. Interseismic coupling and asperity distribution along the Kamchatka subduction zone. J. Geophys. Res. 110, B07405. http://dx.doi.org/10.1029/2005JB003648.
Calmant, S., Pelletier, B., Lebellegard, P., Bevis, M., Taylor, F.W., Phillips, D.A., 2003. New insights on the tectonics along the New Hebrides subduction zone based on GPS results. J. Geophys. Res. 108, 2319. http://dx.doi.org/10.1029/2001JB000644.
Candela, T., Renard, F., Klinger, Y., Mair, K., Schmittbuhl, J., Brodsky, E.E., 2012. Roughness of fault surface over nine decade of length scales. J. Geophys. Res. 117, B08409. http://dx.doi.org/10.1029/2011JB009041.
Chen, T., Lapusta, N., 2009. Scaling of small repeating earthquakes explained by interaction of seismic and aseismic slip in a rate and state fault model. J. Geophys. Res. 114, B01311. http://dx.doi.org/10.1029/2008JB005749.
Chen, T., Newman, A.V., Feng, L., Fritz, H.M., 2009. Slip distribution from the 1 April 2007 Solomon Islands earthquake: a unique image of near-trench rupture. Geophys. Res. Lett. 36, L16307. http://dx.doi.org/10.1029/2009GL039496.

Chester, F.M., Chester, J.S., 1998. Ultracataclasite structure and friction processes of the Punchbowl fault, San Andreas system, California. Tectonophysics 295, 199–221.
Chester, F.M., Chester, J.S., 2000. Stress and deformation along wavy frictional faults. J. Geophys. Res. 105 (B10), 23,421–23,430. http://dx.doi.org/10.1029/2000JB900241.
Chlieh, M., Avouac, J.P., Sieh, K., Natawidjaja, D.H., Galetzka, J., 2008. Heterogeneous coupling of the Sumatran megathrust constrained by geodetic and paleogeodetic measurements. J. Geophys. Res. 113, B05305. http://dx.doi.org/10.1029/2007JB004981.
Chlieh, M., Perfettini, H., Tavera, H., Avouac, J.P., Remy, D., Nocquet, J.M., Rolandone, F., Bondoux, F., Gabalda, G., Bonvalot, S., 2011. Interseismic coupling and seismic potential along the Central Andes subduction zone. J. Geophys. Res. 116, B12405. http://dx.doi.org/10.1029/2010JB008166.
Clift, P.D., Pecher, I., Kukowski, N., Hampel, A., 2003. Tectonic erosion of the Peruvian Forearc, Lima Basin, by subduction and Nazca Ridge collision. Tectonics 22 (3), 1023. http://dx.doi.org/10.1029/2002TC001386.
Cloos, M., 1992. Thrust-type subduction-zone earthquakes and seamount asperities: a physical model for seismic rupture. Geology 20, 601–604.
Cloos, M., Shreve, R.L., 1996. Shear-zone thickness and the seismicity of Chilean- and Marianas-type subduction zones. Geology 24, 107–110.
Cummins, P.R., Baba, T., Kodaira, S., Kaneda, Y., 2002. The 1946 Nankai earthquake and segmentation of the Nankai Trough. Phys. Earth Planet. Inter. 132, 75–87.
Das, S., Watts, A.B., 2009. Effect of subducting seafloor topography on the rupture characteristics of great subduction zone earthquakes. In: Lallemand, S., Funiciello, F. (Eds.), Subduction Zone Geodynamics. Springer-Verlag, Berlin, pp. 103–118.
DeMets, C., Gordon, R.G., Argus, D.F., 2010. Geologically current plate motions. Geophys. J. Int. 181, 1–80. http://dx.doi.org/10.1111/j.1365-246X.2009.04491.x.
Ding, M., Lin, J., 2012. Effects of a subducting seamount on the overriding plate deformation and faulting. American Geophysical Union Fall Meeting, Abstract T11A-2530.
Dominguez, S., Lallemand, S.E., Malavieille, J., von Huene, R., 1998. Upper plate deformation associated with seamount subduction. Tectonophysics 293, 207–224.
Dominguez, S., Malavieille, J., Lallemand, S.E., 2000. Deformation of accretionary wedges in response to seamount subduction: insights from sandbox experiments. Tectonics 19, 182–196.
Doser, D.I., Webb, T.H., 2003. Source parameters of large historical (1917–1961) earthquakes, North Island, New Zealand. Geophys. J. Int. 152, 795–832.
Duan, B., 2012. Dynamic rupture of the 2011 Mw 9.0 Tohoku-Oki earthquake: roles of a possible subducting seamount. J. Geophys. Res. 117, B05311. http://dx.doi.org/10.1029/2011JB009124.
Emry, E.L., Wiens, D.A., Shiobara, H., Sugioka, H., 2011. Seismogenic characteristics of the Northern Mariana shallow thrust zone from local array data. Geochem. Geophys. Geosyst. 12, Q12008. http://dx.doi.org/10.1029/2011GC003853.
Espurt, N., Baby, P., Brusset, S., Roddaz, M., Hermoza, W., Regard, V., Antoine, P.-O., Salas-Gismondi, R., Bolaños, R., 2007. How does the Nazca Ridge subduction influence the modern Amazonian foreland basin? Geology 35, 515–518. http://dx.doi.org/10.1130/G23237A.1.
Fagereng, A., Ellis, S., 2009. On factors controlling the depth of interseismic coupling on the Hikurangi subduction interface, New Zealand. Earth Planet. Sci. Lett. 278, 120–130. http://dx.doi.org/10.1016/j.epsl.2008.11.033.
Fagereng, A., Sibson, R.H., 2010. Melange rheology and seismic style. Geology 38, 751–754.
Faulkner, D.R., Jackson, C.A.L., Lunn, R.J., Schlische, R.W., Shipton, Z.K., Wibberley, C.A.J., Withjack, M.O., 2010. A review of recent developments concerning the structure, mechanics and fluid flow properties of fault zones. J. Struct. Geol. 32, 1557–1575.
Feng, L., Newman, A.V., Protti, M., González, V., Jiang, Y., Dixon, T.H., 2012. Active deformation near the Nicoya Peninsula, northwestern Costa Rica, between 1996 and 2010: interseismic megathrust coupling. J. Geophys. Res. 117, B06407. http://dx.doi.org/10.1029/2012JB009230.
Fisher, M.A., Collot, J.-Y., Geist, E.L., 1991. The collision zone between the North D'Entrecasteaux ridge and the New Hebrides island arc 2. Structure from multichannel seismic data. J. Geophys. Res. 96 (B3), 4479–4495.
Fisher, D.M., Gardner, T.W., Marshall, J.S., Sak, P.B., Protti, M., 1998. Effect of subducting sea-floor roughness on fore-arc kinematics, Pacific Coast, Costa Rica. Geology (Boulder) 26, 467–470.
Fournier, T.J., Freymueller, J.T., 2007. Transition from locked to creeping subduction in the Shumagin region, Alaska. Geophys. Res. Lett. 34 (6), L06303.
Fournier, T., Morgan, J.K., 2012. Insights to slip behavior on rough faults using discrete element modeling. Geophys. Res. Lett. 39, L12304. http://dx.doi.org/10.1029/2012GL015889.
Fryer, P., Smoot, N.C., 1985. Processes of seamount subduction in the Mariana and Izu–Bonin trenches. Mar. Geol. 64, 77–90. http://dx.doi.org/10.1016/0025-3227(85)90161-6.
Fryer, P., Ambos, E.L., Hussong, D.M., 1985. Origin and emplacement of Mariana forearc seamounts. Geology 13, 774–777. http://dx.doi.org/10.1130/0091-7613.
Furlong, K., Lay, T., Ammon, C., 2009. A great earthquake rupture across a rapidly evolving three-plate boundary. Science 324, 226–229. http://dx.doi.org/10.1126/science.1167476.
Gagnon, K., Chadwell, C.D., Norabuena, E., 2005. Measuring the onset of locking in the Peru–Chile trench with GPS and acoustic measurements. Nature 434 (7030), 205–208. http://dx.doi.org/10.1038/nature03412.
Galgana, G., Hamburger, M., McCaffrey, R., Corpuz, E., Chen, Q., 2007. Analysis of crustal deformation in Luzon, Philippines using geodetic observations and earthquake focal mechanisms. Tectonophysics 432, 63–87. http://dx.doi.org/10.1016/j.tecto.2006.12.001.
Gardner, T.W., Fisher, D.M., Morell, K.D., Cupper, M.L., 2013. Upper-plate deformation in response to flat slab subduction inboard of the aseismic Cocos Ridge, Osa Peninsula, Costa Rica. Lithosphere 5 (3), 247–264. http://dx.doi.org/10.1130/L251.1.
Ghosh, A., Newman, A.V., Thomas, A.M., Farmer, G.T., 2008. Interface locking along the subduction megathrust from b-value mapping near Nicoya Peninsula, Costa Rica. Geophys. Res. Lett. 35, L01301. http://dx.doi.org/10.1029/2007GL031617.
Gratier, J.-P., Dysthe, D., Renard, F., 2013a. The role of pressure solution creep in the ductility of the Earth's upper crust. Adv. Geophys. 54. http://dx.doi.org/10.1016/B978-0-12-380940-7.00002-0.
Gratier, J.-P., Thouvenot, F., Jenatton, L., Tourette, A., Doan, M.-L., Renard, F., 2013b. Geological control of the partitioning between seismic and aseismic sliding behaviours in active faults: evidence from the Western Alps, France. Tectonophysics 600, 226–242. http://dx.doi.org/10.1016/j.tecto.2013.02.013.
Gulick, S.P.S., Bangs, N.L., Shipley, T.H., Nakamura, Y., Moore, G.F., Kuramoto, S., 2004. 3-D architecture of the Nankai accretionary prism's imbricate thrust zone off Cape Muroto, Japan: en echelon thrust accommodation of along strike stress regime changes. J. Geophys. Res. 109, B02105. http://dx.doi.org/10.1029/2003JB002654.
Hampel, A., 2002. The migration history of the Nazca Ridge along the Peruvian active margin: a re-evaluation. Earth Planet. Sci. Lett. 203, 665–679.
Hampel, A., Kukowski, N., Bialas, J., Huebscher, C., Heinbockel, R., 2004. Ridge subduction at an erosive margin: the collision zone of the Nazca Ridge in southern Peru. J. Geophys. Res. 109, B02101. http://dx.doi.org/10.1029/2003JB002593.
Hanifa, N.R., Sagiya, T., Kimata, F., Effendi, J., Abidin, H.Z., Meilano, I., 2013. A shallow interplate coupling model in the Java Trench, off the western coast of Java, Indonesia, revealed from GPS data. Japan Geoscience Union Meeting 2013, abstract SSS01-19.
Harpp, K.S., Wanless, V.D., Otto, R.H., Hoernle, K., Werner, R., 2005. The Cocos and Carnegie aseismic ridges: a trace element record of long-term plume-spreading center interaction. J. Petrol. 46 (1), 109–133. http://dx.doi.org/10.1093/petrology/egh064.
Hashimoto, C., Sagiya, T., Matsuura, M., 2009a. Interplate coupling in southwest Japan inferred from GPS data inversion. paper presented at Fall Meeting of Seismological Society of Japan, Kyoto, Abstract A32-08.
Hashimoto, C., Noda, A., Sagiya, T., Matsu'ura, M., 2009b. Interplate seismogenic zones along the Kuril-Japan trench inferred from GPS data inversion. Nat. Geosci. 2, 141–145. http://dx.doi.org/10.1038/NGEO421.
Hayes, D.E., Lewis, S.D., 1984. A geophysical study of the Manila Trench, Luzon, Philippines 1. Crustal structure, gravity, and regional tectonic evolution. J. Geophys. Res. 89, 9171–9195.
Hetland, E.A., Simons, M., 2010. Post-seismic and interseismic fault creep II: transient creep and interseismic stress shadows on megathrusts. Geophys. J. Int. 181, 99–112. http://dx.doi.org/10.1111/j.1365-246X.2009.04482.x.
Heuret, A., Conrad, C.P., Funiciello, F., Lallemand, S., Sandri, L., 2012. Relation between subduction megathrust earthquakes, trench sediment thickness and upper plate strain. Geophys. Res. Lett. 39, L05304. http://dx.doi.org/10.1029/2011GL050712.
Hill, E.M., et al., 2012. The 2010 Mw 7.8 Mentawai earthquake: very shallow source of a rare tsunami earthquake determined from tsunami field survey and near-field GPS data. J. Geophys. Res. 117, B06402. http://dx.doi.org/10.1029/2012JB009159.
Honkura, Y., Nagaya, Y., Kuroki, H., 1999. Effects of seamounts on an interplate earthquake at the Suruga trough, Japan. Earth Planets Space 51, 449–454.
Hsu, Y.J., Yu, S.B., Song, T.R.A., Bacolcol, T., 2012. Plate coupling along the Manila subduction zone between Taiwan and northern Luzon. J. Asian Earth Sci. 51, 98–108. http://dx.doi.org/10.1016/j.jseaes.2012.01.005.
Hu, Y., Wang, K., 2008. Coseismic strengthening of the shallow portion of the subduction fault and its effects on wedge taper. J. Geophys. Res. 113, B12411. http://dx.doi.org/10.1029/2008JB005724.
Huang, Z., Zhao, D., Wang, L., 2011. Seismic heterogeneity and anisotropy of the Honshu arc from the Japan Trench to the Japan Sea. Geophys. J. Int. 184, 1428–1444. http://dx.doi.org/10.1111/j.1365-246X.2011.04934.x.
Ide, S., 2010. Striations, duration, migration and tidal response in deep tremor. Nature 466, 356–360.
Isozaki, Y., Mayuyama, S., Furuoka, F., 1990. Accreted oceanic materials in Japan. Tectonophysics 181, 179–205.
Kato, T., Beavan, J., Matsushima, T., Kotake, Y., Camacho, J.T., Nakao, S., 2003. Geodetic evidence of back-arc spreading in the Mariana Trough. Geophys. Res. Lett. 30 (12), 1625. http://dx.doi.org/10.1029/2002GL016757.
Kelleher, J., McCann, W., 1976. Buoyant zones, great earthquakes, and unstable boundaries of subduction. J. Geophys. Res. 81, 4,885–4,896.
Kimura, G., Ludden, J., 1995. Peeling oceanic crust in subduction zones. Geology 23, 217–220.
Kimura, G., Yamaguchi, A., Hojo, M., Kitamura, Y., Kameda, J., Ujiie, K., Hamada, Y., Hamahashi, M., Hina, S., 2012. Tectonic mélange as fault rock of subduction plate boundary. Tectonophysics 568–569, 25–38. http://dx.doi.org/10.1016/j.tecto.2011.08.025.
King, G., Nábělek, J., 1985. Role of fault bends in the initiation and termination of earthquake rupture. Science 228, 984–987. http://dx.doi.org/10.1126/science.228.4702.984.
Kitamura, Y., Kimura, G., 2012. Dynamic role of tectonic mélange during interseismic process of plate boundary mega earthquakes. Tectonophysics 568–569, 39–52. http://dx.doi.org/10.1016/j.tecto.2011.07.008.
Kluesner, J.W., Silver, E.A., Bangs, N.L., McIntosh, K.D., Gibson, J., Orange, D., Ranero, C.R., von Huene, R., 2013. High density of structurally controlled, shallow to deep water fluid seep indicators imaged offshore Costa Rica. Geochem. Geophys. Geosyst. 14, 519–539. http://dx.doi.org/10.1002/ggge.20058.
Kodaira, S., Takahashi, N., Nakanishi, A., Miura, S., Kaneda, Y., 2000. Subducted seamount imaged in the rupture zone of the 1946 Nankaido earthquake. Science 289, 104–106.
Kodaira, S., No, T., Nakamura, Y., Fujiwara, T., Kaiho, Y., Miura, S., Takahashi, N., Kaneda, Y., Taira, A., 2012. Coseismic fault rupture at the trench axis during the 2011 Tohoku-oki earthquake. Nat. Geosci. 5, 646–650. http://dx.doi.org/10.1038/NGEO1547.
Kopp, H., 2013. The control of subduction zone structural complexity and geometry on margin segmentation and seismicity. Tectonophysics 589, 1–16. http://dx.doi.org/10.1016/j.tecto.2012.12.037.
Kopp, H., Flueh, E.R., Petersen, C.J., Weinrebe, W., Wittwer, A., Meramex, S., 2006. The Java margin revisited: evidence for subduction erosion off Java. Earth Planet. Sci. Lett. 242, 130–142.

Kopp, H., Hindle, D., Klaeschen, D., Oncken, O., Scholl, D., 2009. Anatomy of the western Java plate interface from depth-migrated seismic images. Earth Planet. Sci. Lett. 288, 399–407. http://dx.doi.org/10.1016/j.epsl.2009.09.043.

Kozdon, J.E., Dunham, E.M., 2013. Rupture to the trench: dynamic rupture simulations of the 11 March 2011 Tohoku earthquake. Bull. Seismol. Soc. Am. 103 (2B), 1275–1289. http://dx.doi.org/10.1785/0120120136.

Krabbenhoeft, A., Weinrebe, R.W., Kopp, H., Flueh, E.R., Ladage, S., Papenberg, C., Planert, L., Djajadihardja, Y., 2010. Bathymetry of the Indonesian Sunda margin-relating morphological features of the upper plate slopes to the location and extent of the seismogenic zone. Nat. Hazards Earth Syst. Sci. 10, 1899–1911. http://dx.doi.org/10.5194/nhess-10-1899-2010.

Ku, C.Y., Hsu, S.K., 2008. Crustal structure and deformation at the northern Manila Trench between Taiwan and Luzon islands. Tectonophysics. http://dx.doi.org/10.1016/j.tecto.2007.11.012.

Kumagai, H., Pulido, N., Fukuyama, E., Aoi, S., 2012. Strong localized asperity of the 2011 Tohoku-Oki earthquake, Japan. Earth Planets Space 64, 649–654. http://dx.doi.org/10.5047/eps.2012.01.004.

Kundu, B., Gahalaut, V.K., Catherine, J.K., 2012. Seamount subduction and rupture characteristics of the March 11, 2011, Tohoku earthquake. J. Geol. Soc. India 79 (3), 245–251. http://dx.doi.org/10.1007/s12594-012-0047-6.

LaFemina, P., Dixon, T.H., Govers, R., Norabuena, E., Turner, H., Saballos, A., Mattioli, G., Protti, M., Strauch, W., 2009. Fore-arc motion and Cocos Ridge collision in Central America. Geochem. Geophys. Geosyst. 10, Q05S14. http://dx.doi.org/10.1029/2008GC002181.

Lamb, S., Smith, E., 2013. The nature of the plate interface and driving force of interseismic deformation in the New Zealand plate-boundary zone, revealed by the continuous GPS velocity field. J. Geophys. Res. 118, 3160–3189. http://dx.doi.org/10.1002/jgrb.50221.

Lee, S.J., Huang, B.S., Ando, M., Chiu, H.C., Wang, J.H., 2011. Evidence of large scale repeating slip during the 2011 Tohoku-Oki earthquake. Geophys. Res. Lett. 38, L19306.

Li, F., Sun, Z., Hu, D., Wang, Z., 2013. Crustal structure and deformation associated with seamount subduction at the north Manila Trench represented by analog and gravity modeling. Mar. Geophys. Res. http://dx.doi.org/10.1007/s11001-013-9193-5.

Lockner, D.A., Morrow, C., Moore, D., Hickman, S., 2011. Low strength of deep San Andreas fault gouge from SAFOD core. Nature 472, 82–85. http://dx.doi.org/10.1038/nature09927.

Louat, R., Pelletier, B., 1989. Seismotectonics and present-day relative plate motions in the New Hebrides–North Fiji Basin region. Tectonophysics 167, 41–55.

Loveless, J.P., Meade, B.J., 2010. Geodetic imaging of plate motions, slip rates, and partitioning of deformation in Japan. J. Geophys. Res. 115, B02410. http://dx.doi.org/10.1029/2008JB006248.

Loveless, J.P., Pritchard, M.E., Kukowski, N., 2010. Testing mechanisms of subduction zone segmentation and seismogenesis with slip distributions from recent Andean earthquakes. Tectonophysics 495, 15–33. http://dx.doi.org/10.1016/j.tecto.2009.05.008.

Mahoney, S.H., Wallace, L.M., Miyoshi, M., Villamor, P., Sparks, R.S.J., Hasenaka, T., 2011. Volcano-tectonic interactions during rapid plate-boundary evolution in the Kyushu region, SW Japan. Geol. Soc. Am. Bull. 123, 2201–2223. http://dx.doi.org/10.1130/B30408.1.

Mareschal, J.C., 1989. Fractal reconstruction of sea-floor topography. Pure Appl. Geophys. 131, 197–210.

Marshall, S.T., Morris, A.C., 2012. Mechanics, slip behavior, and seismic potential of corrugated dip slip faults. J. Geophys. Res. 117, B03403. http://dx.doi.org/10.1029/2011JB008642.

Masson, D.G., Parson, L.M., Milsom, J., Nichols, G., Sikumbang, N., Dwiyanto, B., Kallagher, H., 1990. Subduction of seamounts at the Java Trench: a view with long-range sidescan sonar. Tectonophysics 185, 51–65.

McCaffrey, R., 2008. Global frequency of magnitude 9 earthquakes. Geology 36, 263–266.

McCaffrey, R., King, R.W., Payne, S.J., Lancaster, M., 2013. Active tectonics of northwestern U.S. inferred from GPS-derived surface velocities. J. Geophys. Res. 118, 709–723. http://dx.doi.org/10.1029/2012JB009473.

McIntosh, K.D., Silver, E.A., Ahmed, I., Berhorst, A., Ranero, C.R., Kelly, R.K., Flueh, E.R., 2007. The Nicaragua convergent margin: seismic reflection imaging of the source of a tsunami earthquake. In: Dixon, T., Moore, J.C. (Eds.), The Seismogenic Zone of Subduction Thrust Faults. Columbia Univ. Press, New York, pp. 257–287.

Meffre, S., Crawford, A.J., 2001. Collision tectonics in the New Hebrides arc (Vanuatu). Island Arc 10, 33–50.

Megawati, K., Shaw, F., Sieh, K., Huang, Z.H., Wu, T.R., Lin, Y.N., Tan, S.K., Pan, T.C., 2009. Tsunami hazard from the subduction megathrust of the South China Sea: part I. Source characterization and the resulting tsunami. J. Asian Earth Sci. 36, 13–20.

Meltzner, A.J., Sieh, K., Chiang, H.W., Shen, C.C., Suwargadi, B.W., Natawidjaja, D.H., Philibosian, B., Briggs, R.W., 2012. Persistent termini of 2004- and 2005-like ruptures of the Sunda megathrust. J. Geophys. Res. 117, B04405. http://dx.doi.org/10.1029/2011JB008888.

Meneghini, F., Moore, J.C., 2007. Deformation and hydrofracture in a subduction thrust at seismogenic depths: the Rodeo Cove thrust zone, Marin Headlands, California. Geol. Soc. Am. Bull. 119, 174–183. http://dx.doi.org/10.1130/B25807.1.

Mochizuki, K., Yamada, T., Shinohara, M., Yamanaka, Y., Kanazawa, T., 2008. Weak interplate coupling by seamounts and repeating M 7 earthquakes. Science 321, 1194–1197.

Moore, D., Rymer, M.J., 2007. Talc-bearing serpentinite and the creeping section of the San Andreas fault. Nature 448, 795–797. http://dx.doi.org/10.1038/nature06064.

Moreno, M., Melnick, D., Rosenau, M., Bolte, J., Klotz, J., Echtler, H., Baez, J., Bataille, K., Chen, J., Bevis, M., Hase, H., Oncken, O., 2011. Heterogeneous plate locking in the South-Central Chile subduction zone: building up the next great earthquake. Earth Planet. Sci. Lett. 305, 413–424. http://dx.doi.org/10.1016/j.epsl.2011.03.025.

Morgan, E.C., McAdoow, B.G., Baise, L.G., 2008. Quantifying geomorphology associated with large subduction zone earthquakes. Basin Res. 20, 531–542. http://dx.doi.org/10.1111/j.1365-2117.2008.00368.x.

Natawidjaja, D.H., Sieh, K., Ward, S.N., Cheng, H., Edwards, R.L., Galetzka, J., Suwargadi, B.W., 2004. Paleogeodetic records of seismic and aseismic subduction from central Sumatran microatolls, Indonesia. J. Geophys. Res. 109, B04306. http://dx.doi.org/10.1029/2003JB002398.

Natawidjaja, D.H., Sieh, K., Galetzka, J., Suwargadi, B.W., Cheng, H., Edwards, R.L., Chlieh, M., 2007. Interseismic deformation above the Sunda Megathrust recorded in coral microatolls of the Mentawai islands, west Sumatra. J. Geophys. Res. 112, B02404. http://dx.doi.org/10.1029/2006JB004450.

Newcomb, K.R., McCann, W.R., 1987. Seismic history and seismotectonics of the Sunda arc. J. Geophys. Res. 92, 421–439.

Nielsen, S.B., Knopoff, L., 1998. The equivalent strength of geometrical barriers to earthquakes. J. Geophys. Res. 103, 9953–9965.

Nishimura, S., Hashimoto, M., 2006. A model with rigid rotations and slip deficits for the GPS-derived velocity field in southwest Japan. Tectonophysics 421, 187–207. http://dx.doi.org/10.1016/j.tecto.2006.04.017.

Nishizawa, A., Kaneda, K., Watanabe, N., Oikawa, M., 2009. Seismic structure of the subducting seamounts on the trench axis: Erimo Seamount and Daiichi–Kashima Seamount, northern and southern ends of the Japan Trench. Earth Planets Space 61, E5–E8.

Noda, H., Lapusta, N., 2013. Stable creeping fault segments can become destructive as a result of dynamic weakening. Nature 493, 518–521. http://dx.doi.org/10.1038/nature11703.

Norabuena, E., et al., 2004. Geodetic and seismic constraints on some seismogenic zone processes in Costa Rica. J. Geophys. Res. 109, B11403. http://dx.doi.org/10.1029/2003JB002931.

Oakley, A.J., Taylor, B., Moore, G.F., 2008. Pacific Plate subduction beneath the central Mariana and Izu–Bonin fore arcs: new insights from an old margin. Geochem. Geophys. Geosyst. 9, Q06003. http://dx.doi.org/10.1029/2007GC001820.

Oglesby, D.D., Archuleta, R.J., 2003. The three-dimensional dynamics of a nonplanar thrust fault. Bull. Seismol. Soc. Am. 93, 2222–2235.

Okal, E., 2012. The south of Java earthquake of 1921 September 11: a negative search for a large interplate thrust event at the Java Trench. Geophys. J. Int. 190 (3), 1657–1672. http://dx.doi.org/10.1111/j.1365-246X.2012.05570x.

Okamura, Y., 1991. Large-scale melange formation due to seamount subduction: an example from the Mesozoic accretionary complex in central Japan. J. Geol. 99, 661–674.

Okino, K., Ohara, Y., Kasuga, S., Kato, Y., 1999. The Philippine Sea: new survey results reveal the structure and the history of the marginal basins. Geophys. Res. Lett. 26, 2287–2290. http://dx.doi.org/10.1029/1999GL900537.

Pacheco, J.F., Sykes, L.R., Sholz, C.H., 1993. Nature of seismic coupling along simple plate boundaries of subduction type. J. Geophys. Res. 98, 14133–14159.

Park, J.-O., Moore, G.F., Tsura, T., Kodaira, S., Kaneda, Y., 2003. A subducted oceanic ridge influencing the Nankai megathrust earthquake rupture. Earth Planet. Sci. Lett. 217, 77–84.

Park, J.-O., Hori, T., Kaneda, Y., 2009. Seismotectonic implications of the Kyushu–Palau ridge subducting beneath the westernmost Nankai forearc. Earth Planets Space 61, 1013–1018.

Perfettini, H., et al., 2010. Aseismic and seismic slip on the Megathrust offshore southern Peru revealed by geodetic strain before and after the Mw8.0, 2007 Pisco earthquake. Nature 465, 78–81. http://dx.doi.org/10.1038/nature09062.

Power, W., Wallace, L., Wang, X., Reyners, M., 2012. Tsunami hazard posed to New Zealand by the Kermadec and southern New Hebridessubduction margins: An assessment based on plate boundary kinematics, interseismic coupling, and historical seismicity. Pure Appl. Geophys. 169, 1–36. http://dx.doi.org/10.1007/s00024-011-0299-x.

Protti, M., González, V., Newman, A.V., Dixon, T.H., Schwartz, S.Y., Marshall, J.S., Feng, L., Walter, J.I., Malservisi, R., Owen, S.E., 2013. Prior geodetic locking resolved the rupture area of the anticipated 2012 Nicoya earthquake. Nat. Geosci. (in press).

Ranero, C.R., von Huene, R., 2000. Subduction erosion along the Middle America convergent margin. Nature 404, 748–755.

Ranero, C.R., Grevemeyer, I., Sahling, H., Barckhausen, U., Hensen, C., Wallmann, K., Weinrebe, W., Vannucchi, P., von Huene, R., McIntosh, K., 2008. Hydrogeological system of erosional convergent margins and its influence on tectonics and interplate seismogenesis. Geochem. Geophys. Geosyst. 9, Q03S04. http://dx.doi.org/10.1029/2007GC001679.

Rangin, C., Le Pichon, X., Mazzotti, S., Pubellier, M., Chamotrooke, N., Aurelio, M., Walpersdorf, A., Quebral, R., 1999. Plate convergence measured by GPS across the Sundaland/Philippine sea plate deformed boundary: the Philippines and eastern Indonesia. Geophys. J. Int. 139, 296–316.

Rathbun, A., Renard, F., Abe, S., 2013. Numerical investigation of the interplay between wall geometry and friction in fault gouge. J. Geophys. Res. 178, 878–896. http://dx.doi.org/10.1002/jgrb.50106.

Renard, F., Candela, T., Bouchaud, E., 2013. Constant dimensionality of fault roughness from the scale of microfractures to the scale of continents. Geophys. Res. Lett. 40, 83–87. http://dx.doi.org/10.1029/2012GL054143.

Rice, J.M., Cocco, M., 2007. Seismic fault rheology and earthquake dynamics. In: Handy, M.R., Hirth, G., Novius, N. (Eds.), Tectonic Faults: Agents of Change on a Dynamic Earth, Dahlem Workshop Report 95. The MIT Press, Cambridge, MA, pp. 99–138.

Ritz, E., Pollard, D.D., 2012. Stick, slip, and opening of wavy frictional faults: a numerical approach in two dimensions. J. Geophys. Res. 117, B03405. http://dx.doi.org/10.1029/2011JB008624.

Robinson, D.P., Das, S., Watts, A.B., 2006. Earthquake rupture stalled by subducting fracture zone. Science 312, 1203–1205. http://dx.doi.org/10.1126/science.1125771.

Rowe, C.D., Moore, J.C., Remitti, F., the IODP Expedition 343/343T Scientists, 2013. The thickness of subduction plate boundary faults from the seafloor into the seismogenic zone. Geology 41, 991–994. http://dx.doi.org/10.1130/G34556.1.

Ruff, L., 1989. Do trench sediments affect great earthquake occurrence in subduction zones? Pure Appl. Geophys. 129, 263–282.

Ruff, L., Kanamori, H., 1983. Seismic coupling and uncoupling at subduction zones. Tectonophysics 99, 99–117.
Saffer, D., Tobin, H., 2011. Hydrogeology and mechanics of subduction zone forearcs: fluid flow and pore pressure. Annu. Rev. Earth Planet. Sci. 39, 157–186. http://dx.doi.org/10.1146/annurev-earth-040610-133408.
Sagy, A., Brodsky, E.E., 2009. Geometric and rheological asperities in an exposed fault zone. J. Geophys. Res. 114, B02301. http://dx.doi.org/10.1029/2008JB005701.
Sak, P.B., Fisher, D.M., Gardner, T.W., Marshall, J.S., LaFemina, P.C., 2009. Rough crust subduction, forearc kinematics, and Quaternary uplift rates, Costa Rican segment of the Middle American Trench. Geol. Soc. Am. Bull. 121, 992–1012. http://dx.doi.org/10.1130/B26237.1.
Salman, R., Meilano, I., Abidin, H.Z., Sarsito, D., Susilo, S., 2013. Estimation of interplate coupling south of Bali Island, Indonesia, from GPS observations. Abstract SE19-A014, Asia Oceania Geoscience Society Annual Meeting, Brisbane, June 2013.
Sammis, C.G., Steacy, S.J., 1994. The micromechanics of friction in a granular layer. Pure Appl. Geophys. 143, 777–794.
Saucier, F., Humphreys, E., Weldon II, R., 1992. Stress near geometrically complex strike-slip faults: application to the San Andreas Fault at Cajon Pass, southern California. J. Geophys. Res. 97 (B4), 5081–5094. http://dx.doi.org/10.1029/91JB02644.
Scholl, D.W., Kirby, S.H., von Huene, R., 2011. Exploring a link between great and giant megathrust earthquakes and relative thickness of sediment and eroded debris in the subduction channel to roughness of subducted relief. American Geophysical Union Fall Meeting, Abstract T14B–01.
Scholz, C.H., 1998. Earthquakes and friction laws. Nature 391, 37–42.
Scholz, C.H., 2002. The Mechanics of Earthquakes and Faulting, 2nd edition. Cambridge University Press, Cambridge (471 pp.).
Scholz, C.H., Small, C., 1997. The effect of seamount subduction on seismic coupling. Geology 25, 487–490.
Shao, G., Chen, J., Archuleta, R., 2012. Quality of earthquake source models constrained by teleseismic waves: using the 2011 M9 Tohoku-oki earthquake as an example. Poster 93, Presented at Incorporated Research Institutions for Seismology Workshop, Boise, Idaho, June 13–15.
Shiono, K., Mikumo, T., Ishikawa, Y., 1980. Tectonics of the Kyushu–Ryukyu arc as evidenced from seismicity and focal mechanisms of shallow to intermediate-depth earthquakes. J. Phys. Earth 28, 17–43.
Shipton, Z.K., Soden, A.M., Kirkpatrick, J.D., Bright, A.M., Lunn, R.J., 2006. The missing sinks: slip localization in faults, damage zones, and the seismic energy budget. In: Abercrombie, R. (Ed.), Earthquakes: Radiated Energy and the Physics of Faulting, Geophysical Monograph Series 170. America Geophysical Union, Washington DC, pp. 193–198. http://dx.doi.org/10.1029/170GM22.
Shulgin, A., Kopp, H., Mueller, C., Planert, L., Lueschen, E., Flueh, E.R., Djajadihardja, Y., 2011. Structural architecture of oceanic plateau subduction offshore Eastern Java and the potential implications for geohazards. Geophys. J. Int. 184, 12–28.
Sibson, R.H., 1985. Stopping of earthquake ruptures at dilatational fault jogs. Nature 316, 248–251.
Sibson, R.H., 2003. Thickness of the seismic slip zone. Bull. Seismol. Soc. Am. 93, 1169–1178.
Sibson, R.H., 2013. Stress switching in subduction forearcs: implications for overpressure containment and strength cycling on megathrusts. Tectonophysics 600, 142–152. http://dx.doi.org/10.1016/j.tecto.2013.02.035.
Singh, S.C., Hananto, N., Mukti, M., Robinson, D.P., Das, S., Chauhan, A., Carton, H., Gratacos, B., Midnet, S., Djajadihardja, Y., Harjono, H., 2011. Aseismic zone and earthquake segmentation associated with a deep subducted seamount in Sumatra. Nat. Geosci. 4, 308–311.
Sparkes, R., Tilmann, F., Hovius, N., Hillier, J., 2010. Subducted seafloor relief stops rupture in South American great earthquakes: implications for rupture behaviour in the 2010 Maule, Chile earthquake. Earth Planet. Sci. Lett. 298, 89–94. http://dx.doi.org/10.1016/j.epsl.2010.07.029.
Stein, S., Okal, E.A., 2007. Ultralong period seismic study of the December 2004 Indian Ocean earthquake and implications for regional tectonics and the subduction process. Bull. Seismol. Soc. Am. 97, S279–S295. http://dx.doi.org/10.1785/0120050617.
Suito, H., Freymueller, J.T., 2009. A viscoelastic and afterslip postseismic deformation model for the 1964 Alaska earthquake. J. Geophys. Res. 114, B11404. http://dx.doi.org/10.1029/2008JB005954.
Suwa, Y., Miura, S., Hasegawa, A., Sato, T., Tachibana, K., 2006. Interplate coupling beneath NE Japan inferred from three-dimensional displacement field. J. Geophys. Res. 111, B04402. http://dx.doi.org/10.1029/2004JB003203.
Swenson, J.L., Beck, S.L., 1996. Historical 1942 Ecuador and 1942 Peru subduction earthquakes, and earthquake cycles along Colombia Ecuador and Peru subduction segments. Pure Appl. Geophys. 146 (1), 67–101.
Swenson, J.L., Beck, S.L., 1999. Source characteristics of the 12 November 1996 M-w 7.7 Peru subduction zone earthquake. Pure Appl. Geophys. 154 (3–4), 731–751.
Taylor, B., Hayes, D.E., 1983. Origin and history of the South China Basin. In: Hayes, D.E. (Ed.), The Tectonic and Geologic Evolution of Southeast Asian Seas and Islands, Geophysical Monograph 23. American Geophysical Union, Washington, D.C., pp. 89–104.
Titus, S.J., DeMets, C., Tikoff, B., 2006. Thirty-five-year creep rates for the creeping segment of the San Andreas fault and the effects of the 2004 Parkfield earthquake: constraints from alignment arrays, continuous global positioning system, and creepmeters. Bull. Seismol. Soc. Am. 96, S250–S268. http://dx.doi.org/10.1785/0120050811.
Tsuru, T., Park, J.O., Miura, S., Kodaira, S., Kido, Y., Hayashi, T., 2002. Along-arc structural variation of the plate boundary at the Japan Trench margin: implication of interplate coupling. J. Geophys. Res. 107, 2357. http://dx.doi.org/10.1029/2001JB001664.
Turcotte, D.L., 1992. Fractals and Chaos in Geology and Geophysics. Cambridge University Press, Cambridge (221 pp.).
Uchida, N., Matsuzawa, T., 2011. Coupling coefficient, hierarchical structure, and earthquake cycle for the source area of the 2011 off the Pacific coast of Tohoku earthquake inferred from small repeating earthquake data. Earth Planets Space 63, 675–679. http://dx.doi.org/10.5047/eps.2011.07.006.
Uchida, N., Nakajima, J., Hasegawa, A., Matsuzawa, T., 2009. What controls interplate coupling?: evidence for abrupt change in coupling across a border between two overlying plates in the NE Japan subduction zone. Earth Planet. Sci. Lett. 283, 111–121.
Uchida, N., Kirby, S.H., Okada, T., Hino, R., Hasegawa, A., 2010. Supraslab earthquake clusters above the subduction plate boundary offshore Sanriku, northeastern Japan: Seismogenesis in a graveyard of detached seamounts? J. Geophys. Res. 115, B09308. http://dx.doi.org/10.1029/2009JB006797.
Ueda, H., 2005. Accretion and exhumation structures formed by deeply subducted seamounts in the Kamuikotan high-pressure/temperature zone, Hokkaido, Japan. Tectonics 24, TC2007. http://dx.doi.org/10.1029/2004TC001690.
Uyeda, S., Kanamori, H., 1979. Back-arc opening and the mode of subduction. J. Geophys. Res. 84 (B3), 1049–1061. http://dx.doi.org/10.1029/JB084iB03p01049.
Vannucchi, P., Fisher, D.M., Bier, S., Gardner, T.W., 2006. From seamount accretion to tectonic erosion: formation of Osa Melange and the effects of Cocos Ridge subduction in southern Costa Rica. Tectonics 25, TC2004. http://dx.doi.org/10.1029/2005TC001855.
von Huene, R., 2008. Geophysics — when seamounts subduct. Science 321, 1165–1166.
von Huene, R., Scholl, D., 1991. Observations at convergent margins concerning sediment subduction, subduction erosion, and the growth of continental crust. Rev. Geophys. 29, 279–316.
von Huene, R., Ranero, C.R., Weinrebe, W., Hinz, K., 2000. Quaternary convergent margin tectonics of Costa Rica, segmentation of the Cocos Plate and Central American volcanism. Tectonics 19, 314–334.
Wada, I., Wang, K., 2009. Common depth of slab-mantle decoupling: reconciling diversity and uniformity of subduction zones. Geochem. Geophys. Geosyst. 10, Q10009.
Wakida, K., 2012. Mappable features of mélanges derived from Ocean Plate Stratigraphy in the Jurassic accretionary complexes of Mino and Chichibu terranes in Southwest Japan. Tectonophysics 568–569, 74–85. http://dx.doi.org/10.1016/j.tecto.2011.10.019.
Wallace, L.M., Beavan, J., 2010. Diverse slow slip behavior at the Hikurangi subduction margin, New Zealand. J. Geophys. Res. 115, B12402. http://dx.doi.org/10.1029/2010JB007717.
Wallace, L.M., Beavan, J., McCaffrey, R., Darby, D., 2004. Subduction zone coupling and tectonic block rotations in the North Island, New Zealand. J. Geophys. Res. 109, B12406. http://dx.doi.org/10.1029/2004JB003241.
Wallace, L.M., Ellis, S., Miyao, K., Miura, S., Beavan, J., Goto, J., 2009a. Enigmatic, highly active left-lateral shear zone in southwest Japan explained by aseismic ridge collision. Geology 37, 143–146. http://dx.doi.org/10.1130/G25221A.1.
Wallace, L.M., et al., 2009b. Characterizing the seismogenic zone of a major plate boundary subduction thrust: Hikurangi margin, New Zealand. Geochem. Geophys. Geosyst. 10, Q10006. http://dx.doi.org/10.1029/2009GC002610.
Wallace, L.M., Fagereng, A., Ellis, S., 2012. Upper plate tectonic stress state may influence interseismic coupling on subduction megathrusts. Geology 40, 895–898. http://dx.doi.org/10.1130/G33373.1.
Wang, K., 2007. Elastic and viscoelastic models of subduction earthquake cycles. In: Dixon, T., Moore, C. (Eds.), The Seismogenic Zone of Subduction Thrust Faults. Columbia University Press, pp. 540–575.
Wang, K., 2011. Coseismic fault slip in the Tohoku-Oki earthquake: how large and how close to the trench? American Geophysical Union Fall Meeting, Abstract G51A–0852.
Wang, K., Bilek, S.L., 2011. Do subducting seamounts generate or stop large earthquakes? Geology 39, 819–822. http://dx.doi.org/10.1130/G31856.1.
Wang, K., Wells, R., Mazzotti, S., Hyndman, R.D., Sagiya, T., 2003. A revised dislocation model of interseismic deformation of the Cascadia subduction zone. J. Geophys. Res. 108, 2026. http://dx.doi.org/10.1029/2001JB001227.
Wang, K., Hu, Y., He, J., 2012. Deformation cycles of subduction earthquakes in a viscoelastic Earth. Nature 484, 327–332. http://dx.doi.org/10.1038/nature11032.
Watts, A.B., Koppers, A.A.P., Robinson, D.P., 2010. Seamount subduction and earthquakes. Oceanography 23, 166–173.
Webb, T., Anderson, H., 1998. Focal mechanisms of large earthquakes in the North Island of New Zealand: Slip partitioning at an oblique active margin. Geophys. J. Int. 134 (1), 40–86. http://dx.doi.org/10.1046/j.1365-246x.1998.00531.x.
Wei, S., Graves, R., Helmberger, D.V., Avouac, J.-P., Jiang, J., 2012. Sources of shaking and flooding during the Tohoku-Oki earthquake: a mixture of rupture styles. Earth Planet. Sci. Lett. 333–334, 91–100. http://dx.doi.org/10.1016/j.epsl.2012.04.006.
Wesnousky, S.G., 1988. Seismological and structural evolution of strike–slip faults. Nature 335, 340–343.
Wesnousky, S.G., 2006. Predicting the endpoints of earthquake ruptures. Nature 444, 358–360.
Wibberley, C.A.J., Yielding, G., Di Toro, G., 2008. Recent development in the understanding of fault zone internal structure: a review. In: Wibberley, C.A.K., Kurz, W., Imber, J., Holdsworth, R.E., Collettini, C. (Eds.), The Internal Structure of Fault Zones: Implications for mechanical and Fluid-flow Properties. The Geological Society of London, 299, pp. 5–33.
Wu, T.R., Huang, H.C., 2009. Modeling tsunami hazards from Manila trench to Taiwan. J. Asian Earth Sci. 36, 21–28.
Yagi, Y., Kikuchi, M., Yoshida, S., Yamanaka, Y., 1998. Source process of the Hyuga-nada earthquake of April 1, 1968 (MJMA 7.5), and its relationship to the subsequent seismicity (in Japanese with English abstract). Zisin 51, 139–148.
Yamamoto, Y., Obana, K., Takahashi, T., Nakanishi, A., Kodaira, S., Kaneda, Y., 2013. Imaging of the subducted Kyushu–Palau Ridge in the Hyuga-nada region, western Nankai

Trough subduction zone. Tectonophysics 589, 12–90. http://dx.doi.org/10.1016/j.tecto.2012.12.028.
Yamanaka, Y., Kikuchi, M., 2004. Asperity map along the subduction zone in northeastern Japan inferred from regional seismic data. Geophys. J. Int. 109, B07307. http://dx.doi.org/10.1029/2003JB002683.
Yang, H., Liu, Y., Lin, J., 2012. Effects of subducted seamounts on megathrust earthquake nucleation and rupture propagation. Geophys. Res. Lett. 39, L24302. http://dx.doi.org/10.1029/2012GL053892.
Yang, H., Liu, Y., Lin, J., 2013. Geometrical effects of a subducted seamount on stopping megathrust ruptures. Geophys. Res. Lett. 40, 2011–2016. http://dx.doi.org/10.1002/grl.50509.
Yoshioka, S., Matsuoka, Y., 2013. Interplate coupling along the Nankai Trough, southwest Japan, inferred from inversion analyses of GPS data: effects of subducting plate geometry and spacing of hypothetical ocean-bottom GPS stations. Tectonophysics 600, 165–174. http://dx.doi.org/10.1016/j.tecto.2013.01.023.
Yu, S.B., Hsu, Y.J., Bacolcol, T., Yang, C.C., Tsai, Y.C., Solidum, R., 2013. Present-day crustal deformation along the Philippine fault in Luzon, Philippines. J. Asian Earth Sci. 65, 64–74. http://dx.doi.org/10.1016/j.jseaes.2010.12.007.
Zhao, D., Huang, Z., Umino, N., Hasegawa, A., Kanamori, H., 2011. Structural heterogeneity in the megathrust zone and mechanism of the 2011 Tohoku-oki earthquake (Mw 9.0). Geophys. Res. Lett. 38, L17308. http://dx.doi.org/10.1029/2011GL048408.
Zhu, J., Kopp, H., Flueh, E.R., Klaeschen, D., Papenberg, C., Planert, L., 2009. Crustal structure of the central Costa Rica subduction zone: implications for basal erosion from seismic wide-angle data. Geophys. J. Int. 178, 1112–1131. http://dx.doi.org/10.1111/j.1365-246X.2009.04208.x.